NASA TECHNICAL MEMORANDUM 100599

STRESS-INTENSITY FACTORS FOR SMALL SURFACE AND CORNER CRACKS IN PLATES

I. S. Raju, S. N. Atluri, and J. C. Newman, Jr.

APRIL 1988

NASA

National Aeronautics and Space Administration

Langley Research Center
Hampton, Virginia 23665

STRESS-INTENSITY FACTORS FOR SMALL SURFACE AND CORNER CRACKS IN PLATES

I. S. Raju, S. N. Atluri, and J. C. Newman, Jr.
NASA Langley Research center
Hampton , Va 23665-5225

ABSTRACT

Three-dimensional finite-element and finite-element-alternating methods were used to obtain the stress-intensity factors for small surface and corner cracked plates subjected to remote tension and bending loads. The crack-depth-to-crack-length ratios (a/c) ranged from 0.2 to 1 and the crack-depth-to-plate-thickness ratios (a/t) ranged from 0.05 to 0.2. The performance of the finite-element alternating method was studied on these crack configurations. A study of the computational effort involved in the finite-element alternating method showed that several crack configurations could be analyzed with a single rectangular mesh idealization, whereas the conventional finite-element method requires a different mesh for each configuration. The stress-intensity factors obtained with the finite-element-alternating method agreed well (within 5 percent) with those calculated from the finite-element method with singularity elements.

The stress-intensity factors calculated from the empirical equations proposed by Newman and Raju were generally within 5 percent of those calculated by the finite-element method. The stress-intensity factors given herein should be useful in predicting crack-growth rates and fracture strengths of surface- and corner-cracked components.

KEY WORDS: Crack, elastic analysis, stress-intensity factor, finite-element method, finite-element-alternating method, surface crack, corner crack, tension and bending loads.

INTRODUCTION

Surface and corner cracks may occur in many structural components. These cracks initiate near regions of stress concentrations and may cause premature failure of aircraft landing gears, spars, stiffeners, and other components [1]. Accurate stress-intensity factor solutions for these components are needed for reliable prediction of crack-growth rates and fracture strengths.

Most of the life of these cracked components is spent when the cracks are small. Also, many applications of damage tolerance or durability analyses require the computation of stress-intensity factors for small cracks. Previous analyses of surface- and corner-crack configurations, using three-dimensional finite-element analyses [2-4], boundary-integral equation methods [5], and alternating methods [6-8] have considered crack-depth-to-plate-thickness ratios greater than or equal to 0.2. Engineering judgment or extrapolations were used to estimate stress-intensity factors for small surface and corner cracks [9,10]. Therefore, more analyses are needed to verify these extrapolations for small cracks. The purpose of this paper is to present stress-intensity factors for a wide range of semi-elliptical surface cracks and quarter-elliptical corner cracks in plates with crack-depth-to-plate-thickness ratios less than 0.2 and obtain asymptotic values as crack-depth-to-plate thickness ratios approach zero.

Two popular methods to obtain the stress-intensity factors for the surface- and corner-crack configurations are the finite-element method with singularity elements [2-4] and the finite-element-alternating method [11-13]. In the finite-element method, large number of elements are needed with customized modeling near the crack front with singularity elements. Once such models are developed, accurate stress-intensity factors can be obtained [2-4]. In contrast, the finite-element-alternating method does not need customized modeling near the crack front. This is because the uncracked solid is analyzed by the finite-element part of the method. The second objective of this paper is to study various types of modeling that could be used and to study the computational efficiency of the method. The stress-intensity factors obtained with the finite-element-alternating method were compared with those from the finite-element method with singularity elements for surface- and corner-crack configurations. The stress-intensity factors obtained by these methods were also compared with values calculated from empirical equations for surface- and corner-cracked plates with crack-depth-to-plate-thickness ratios less than 0.2.

ANALYSIS

Two types of crack configurations: a surface- and corner-cracked plate, as shown in Figure 1, were analyzed. The three-dimensional finite-element method and finite-element-alternating method were used to obtain the mode I stress-intensity factors. In these analyses, Poisson's ratio (ν) was assumed to be 0.3.

Loading

Two types of loading were applied to the crack configurations: remote uniform tension and remote out-of-plane bending (bending about the x-axis). The remote uniform tensile stress is S_t in the z-direction and the remote outer-fiber bending stress is S_b. The bending stress S_b is the outer fiber stress calculated at the origin (x = y = z = 0 in Fig. 1) without the crack present.

Stress-Intensity Factor

The tensile and bending loads cause only mode I deformations. The mode I stress-intensity factor K for any point along the crack front was taken to be

$$K = S_i \left(\pi a/Q \right)^{1/2} . F(a/t, a/c, \phi) \qquad (1)$$

where the subscript i denotes tension load (i = t) or bending load (i = b), a is the crack depth, c is the surface length, t is the thickness of the plate, ϕ is the parametric angle of the ellipse, and Q is the shape factor of the ellipse (which is equal to the square of the complete elliptic integral of the second kind). The half length of the bar, h, and the width , b, (see Fig. 1) were chosen large enough (h/b >2 and b/c > 5) to have negligible effects on the stress-intensity factors. Values of F, the boundary-correction factor, were calculated along the crack front for various crack shapes (a/c = 0.2 to 1) with a/t values of 0.05, 0.1, and 0.2. The crack dimensions and the parametric angle are defined in Figures 1 and 2.

Three-Dimensional Finite-Element Method

Figure 3 shows a typical finite-element model for a surface or corner crack in a rectangular plate. The same finite-element model was used to obtain the stress-intensity factors for the surface- and corner-crack configurations. For the surface-crack configuration, symmetric boundary conditions were imposed on the $z = 0$ and $x = 0$ planes. Whereas, for the corner-crack configuration, symmetric boundary conditions were imposed only on the $z = 0$ plane. The finite-element models employed six-noded, pentahedron, singularity elements at the crack front and eight-noded, hexahedral elements elsewhere. Stress-intensity factors were evaluated using the nodal-force method [2]. Details of the formulation of these types of elements and development of the finite-element models are given in references 2 through 4 and are not repeated here.

Finite-Element-Alternating Method

This method is based on the Schwartz-Neumann alternating technique. The alternating method uses two basic solutions of elasticity and alternates between these two solutions to satisfy the required boundary conditions of the cracked body [6-8]. One of the solutions is for the stresses in an uncracked finite solid, and the other is for the stresses in an infinite solid with a crack subjected to arbitrary normal and shear tractions. The solution for an uncracked body may be obtained in several ways, such as the finite- element method or the boundary-element method. In this paper, the three-dimensional finite-element method was used.

The procedure that is followed in the alternating method is summarized in the flow chart in Figure 4 and is briefly explained here for mode-I problems. First, solve the uncracked solid subjected to the given external loading using the three-dimensional finite-element method (Step 1 in Fig.4). The finite-element solution gives the stresses everywhere in the solid including the region over which the crack is present (Step 2). The normal stresses acting on the region of the crack need to be erased to satisfy the crack-boundary conditions. The opposite of the stresses calculated in Step 2 are fit to an nth degree polynomial in terms of x- and z-coordinates (Step 4). Due to the polynomial stress distributions obtained in Step 4, calculate the stress-intensity factor [11] for the current iteration (Step 5). Use the analytical solution of an embedded elliptic crack in a infinite solid subjected to the polynomial normal traction [11] to obtain the normal and tangential stresses on all the external surfaces of the solid (Step 6). The opposite of these stresses on the external surfaces obtained in Step 6 are then considered as the externally prescribed stresses on the uncracked solid (Step 7). Again, solve the uncracked solid problem due to the surface tractions calculated in Step 7. This is the start of the next iteration. Continue this iteration process until the normal stresses in the region of the crack are negligibly small or lower than a prescribed tolerance level. The stress-intensity factors in the converged solution are simply the sum of the stress-intensity factors, that are computed in Step 5, from all iterations.

The key element in the alternating method is, obviously, the analytical solution for an infinite solid with an embedded elliptical crack

subjected to arbitrary normal and shear tractions. Such a solution was first obtained by Shah and Kobayashi [14] for tractions normal to the crack surface. However, this solution was limited to a third-degree polynomial function in each of the Cartesian coordinates describing the ellipse. Vijayakumar and Atluri [15] overcame this limitation and obtained a general solution of arbitrary polynomial order. Nishioka and Atluri [11-13] improved and implemented this general solution in a finite-element-alternating method and analyzed surface- and corner-cracked plates. The details of the method are well documented in references 11 through 13 but they are briefly described herein.

In the 3-D finite-element solution, twenty-noded isoparametric parabolic elements were used to model the uncracked solid. Two types of idealizations were used. In the first type, the idealization was such that the elements on the $z = 0$ plane conform to the shape of the crack in the cracked solid (see Fig. 5(a)). Although the finite-element solution is for the uncracked body, such an idealization is convenient to perform the polynomial fit using the finite-element stresses from the elements that are contained in the region of the crack. The 3-D mesh is then generated by simply translating in the z- direction the mesh on the $z = 0$ plane. These models will be referred to as the mapped models. A typical mapped model is shown in Figure 5(a). In the second type, simple rectangular idealizations were used to model the solid. These models are referred to as the rectangular models. A typical rectangular model is shown in Figure 5(b).

The alternating method requires a fit to the stresses, obtained from

the finite-element solution (of the uncracked body), at the crack location (Step 4). These stresses are the residual pressures that need to be erased. For corner cracks, the residual crack-face pressure distribution, σ^R_z, was assumed to be a complete fifth-degree polynomial in x and y with 21 terms as shown in the Pascal's triangle below.

$$
\begin{array}{ccccccccccc}
 & & & & & 1 & & & & & \\
 & & & & x & & y & & & & \\
 & & & x^2 & & xy & & y^2 & & & \\
 & & x^3 & & x^2y & & xy^2 & & y^3 & & \\
 & x^4 & & x^3y & & x^2y^2 & & xy^3 & & y^4 & \\
x^5 & & x^4y & & x^3y^2 & & x^2y^3 & & xy^4 & & y^5
\end{array}
$$

For surface cracks, the residual pressure σ^R_z had only 12 terms because of symmetry about the y-axis. These twelve terms were obtained by neglecting the terms involving odd powers of x in the fifth-degree polynomial shown in the Pascal's triangle. For mapped models, the residual pressure was fit over the complete region of the crack. For rectangular models, the residual pressure was fit over a rectangular region bounded by the semi-minor and semi-major axes of the crack (see shaded region in Fig. 6).

Because the continuum solution corresponds to that of an embedded elliptic crack in an infinite solid, it is necessary to define the residual stresses not only on the region of the crack but also on the "fictitious" portion of the crack which lies outside of the finite solid. Nishioka and Atluri [11-13] suggested the residual-pressure distribution, through numerical experimentation, to be

$$\sigma^R_z = \begin{cases} \sigma^R_z\,(0,y) & \text{for } x \le 0,\ y \ge 0 \\ \sigma^R_z\,(0,0) & \text{for } x \le 0,\ y \le 0 \\ \sigma^R_z\,(x,0) & \text{for } x \ge 0,\ y \le 0 \end{cases}$$

for corner cracks, and

$$\sigma^R_z = \sigma^R_z\,(x,0) \quad \text{for } x \ge 0,\ y \le 0$$

for surface cracks.

The stresses computed at the nodal points of a 20-node element in a finite-element analysis can be be inaccurate [16]. Therefore, the stresses were evaluated at the 2x2x2 Gaussian points of an element and then were extrapolated to the element nodes as suggested by Hinton et al [16,17].

RESULTS AND DISCUSSION

In this section, the convergence of the finite-element-alternating method is studied. Then, the stress-intensity factors obtained from this method are compared to those calculated by the three-dimensional finite-element method. Next, the stress-intensity factors for various crack configurations are compared to those calculated from empirical stress-intensity factor equations.

Convergence of the Finite-Element-Alternating Method

To study the convergence of the finite-element-alternating method, an oblong corner crack subjected to remote uniform tension with an a/c ratio of 0.2 was considered. The corner-crack configuration was chosen because the

configuration is more severe than the surface-crack configuration because of the existence of an additional free surface (x = 0 plane). The a/c ratio of 0.2 was chosen because larger areas of the external surfaces need to be made stress free.

Figure 7(a) shows a typical mapped model on the z = 0 plane for a shallow corner crack (a/t = 0.2) with 20-noded isoparametric elements. This coarse model had 982 nodes and 162 elements and uses 4 elements to model region corresponding to the crack face. Two other models, medium and fine, using 8- and 12-elements to model the region corresponding to the crack face, see Figure 7(b) and 7(c), respectively. All three models had 9 unequal layers of elements in the height (z) direction. For all three models, the stress-intensity factors converged to within one-percent accuracy in 5 iterations. The average residual pressure on the crack face normalized by the remote tension stress showed excellent convergence, as shown in Table 1.

Figure 8 presents the normalized stress-intensity factors all along the crack front for the three models. The stress-intensity factors from the three models agreed well with one another and indicated that even coarse models give accurate results.

Figure 9 shows the three rectangular models (on the z = 0 plane) that were used in the analyses: coarse, medium and fine. The three models were developed such that the coarse model is a subset of the medium and the medium model is a subset of the fine model. All models had the same

refinement in the height (z) direction. The coarse and medium models had only 4 elements, while the fine model had 9 elements in the crack region. The coarse model had only 5 elements in the y-direction while the medium model had 7 elements in the y-direction. In both cases the x-refinement was held constant. The fine mesh, on the other hand, had 9 elements in the y-direction and 7-elements in the x-direction. Therefore, the fine model had better refinement near the crack front. The plate was idealized with 175, 245, and 441 elements for the coarse, medium and fine models, respectively. For these models, the stress-intensity factors converged to within one-percent accuracy in 4 iterations. The average residual pressure on the crack face normalized by the remote uniform tension stress, again, showed excellent convergence, as shown in the Table 2.

Figure 10 presents the normalized stress-intensity factors obtained from the three rectangular models for a slightly different corner-crack configuration ($a/c = 0.2$ and $a/t = 0.1$) than used for the mapped models. Small differences in stress-intensity factors were found between the medium and fine models (about 0.5 percent). However, for larger values of ϕ considerable differences were observed between the coarse and medium models. This behavior was caused by inadequate refinement in the y-direction for the coarse model. These results suggest that accurate stress-intensity factors can be obtained from rectangular models with as little as 4 elements in the region of the crack, provided adequate refinement is used in modeling the free surfaces.

Comparison of Stress-intensity Factors

Figures 11 and 12 compare the stress-intensity factors for shallow corner cracks (a/c = 0.2) obtained with the finite-element method and the finite-element-alternating method for a/t = 0.2 and 0.1, respectively. The results from the mapped and rectangular (medium) models are shown in Figure 11, while the results from a rectangular (medium) model are shown in Figure 12. The results shown from both analyses in Figure 11 agreed well. The maximum difference was near $\phi = 0$ and was about 4 percent. (Herein, "percent difference" is defined as the difference between the two solutions normalized by the largest value for that configuration.) Figure 12 shows that the results from the rectangular model agreed well with those obtained from the finite-element method, except near $\phi = 0$. The maximum difference, however, was about 6 percent.

Figures 13 and 14 present comparisons of stress-intensity factors for a nearly semi-circular surface crack and nearly quarter-circular corner crack, respectively, obtained with the finite-element method and the finite-element-alternating method. Note that the finite-element-alternating method cannot be used for cracks with an a/c ratio of unity because the elliptic functions have indefinite forms. From numerical experimentation the limiting values of the a/c ratio appear to be 0.98 for embedded cracks, 0.92 for surface cracks, and 0.85 for corner cracks. Thus, an a/c value of 0.85 was chosen for both crack configurations. These figures show reasonable agreement between the two methods for both the surface- and corner-crack configurations. The largest discrepancy occurred where the crack front intersects a free surface (about 5 percent).

Computational Effort of the Finite-Element-Alternating Method

A study of the computational time for the alternating method indicated that assembling and decomposing the finite-element stiffness matrix was the most dominant computational effort. Each iteration was approximately *one percent* of the time required to assemble and decompose the stiffness matrix. For the configurations studied, convergence to less than one percent error bound in the stress-intensity factors was achieved in 4 or 5 iterations. The results shown in Figure 12 suggest that rectangular models provide accurate solutions and these models are easier to generate than the mapped models. The rectangular models give accurate results provided that adequate refinement is made along each coordinate axis. Most importantly, a single rectangular fine mesh can be used to analyze a wide range of crack shapes and sizes without repeated assembly and decomposition of the stiffness matrix. For example, the computational time required to analyze three crack shapes (a/c) and three crack sizes (a/t), or 9 crack configurations, using the finite-element-alternating method was 630 CPU seconds (VPS-32 Computer). The conventional finite-element method requires nine separate computer runs. The computational time for one run was about 400 CPU seconds (VPS-32 Computer). Therefore, 3600 CPU seconds are required for the finite-element method.

Stress-Intensity Factors for Small Cracks

Stress-intensity factor equations [9,10] have been developed by using the stress-intensity factors obtained from the finite-element method, engineering judgement, and extrapolations. To evaluate the equations for $a/t < 0.2$, therefore, it is logical that the values from the equation be

compared with those from the finite-element method. Furthermore, the differences between the results from the finite-element-alternating method and the finite-element method with singularity elements were about 3 percent for most of the crack front. Therefore, stress-intensity factors were calculated for various crack shapes (a/c = 0.2 to 1) with a/t ratios ranging from 0.05 to 0.2 by using the finite-element method. A typical stress-intensity factor distribution for a corner crack with a/c = 0.4, subjected to remote uniform tension loading, for various a/t ratios are shown in Figure 15. For remote tensile loading and all a/c ratios considered, smaller a/t values always gave slightly lower stress-intensity factors all along the crack front. However, the difference in stress-intensity factors from an a/t value of 0.2 to 0.05 was less than 3 percent. For remote bending loading and all a/c ratios, smaller values of a/t gave higher stress-intensity factors all along the crack front. This is expected because the crack experiences a more uniform stress gradient as a/t approaches zero. At a/t = 0, the bending stress-intensity correction factors (F) are exactly equal to those due to remote tension. At a/t = 0.05, the maximum differences between the stress-intensity correction factors at the deepest point of the crack due to remote tension and remote bending loading are about 10 percent.

The present results were also compared to the empirical stress-intensity factor equations proposed by Newman and Raju [9,10]. As previously mentioned, the empirical equations were obtained by a curve fitting procedure to the finite-element results in the range $0.2 \leq a/t \leq 0.8$ for various crack shapes. In developing the empirical equations, some engineering judgment and extrapolations were used for the limiting solution

for a/t = 0. The present finite-element results are compared with calculations from the empirical equations in Figures 16 through 19 for surface or corner cracks. For surface cracks, the comparisons were made at the maximum depth point ($2\phi/\pi = 1$) and near the free surface ($2\phi/\pi = 0.125$) for the surface crack. At the free surface ($2\phi/\pi = 0$), the finite-element results are influenced by the boundary-layer effect and the results are mesh dependent [2]. For corner cracks, the comparisons are also made near the two free surfaces ($2\phi/\pi = 0.125$ and 0.875). The results from the empirical equations (solid curves) are generally within about 5 percent of the finite-element results for the range of a/c ratios considered.

From the finite element results, asymptotic stress-intensity correction values at a/t = 0 were computed by fitting a quadratic equation in terms of a/t to the results for a/t values of 0.2, 0.1, 0.05. These asymptotic values (average of the tension and bending loads) are shown in Table 3. These values are also compared with those obtained from the empirical equations. The asymptotic values from the empirical equation and the extrapolated finite-element results at a/t = 0 agreed well (within 3 percent). Thus, the empirical equations have an accurate limit as a/t approaches zero.

CONCLUDING REMARKS

Stress-intensity factors for shallow surface and corner cracks in rectangular plates were obtained using the three-dimensional finite-element and finite-element-alternating methods. The plates were subjected to remote

tension and remote out-of-plane bending loads. A wide range of crack shapes were considered (a/c = 0.2 to 1). The crack-depth-to-plate-thickness (a/t) ratios ranged from 0.05 to 0.2.

The performance of the finite-element-alternating method was studied by considering two types of models: mapped and rectangular models. The mapped models used idealizations that conform to the shape of the crack while the rectangular models used a rectangular idealization throughout the solid. The stress-intensity factors obtained by either model showed excellent convergence and showed that about 4 to 8 elements are sufficient to model the crack region. The stress-intensity factors obtained from the finite- element-alternating method agreed well with those obtained the finite-element method with singularity elements (maximum difference was about 5 percent.) The study of the computational effort involved in the finite-element-alternating method showed that a single rectangular idealization could be used to analyze several crack configurations. The method produced accurate stress-intensity factors at a lower cost compared to the conventional finite-element method.

For remote tensile loading and all crack shapes (crack depth-to-surface-length ratios, a/c) considered, lower values of the crack-depth-to-plate-thickness (a/t) ratios gave lower stress-intensity factors for surface- and corner-cracked plates. However, the largest difference between the stress-intensity factors for a/t values ranging from 0.05 to 0.2 was only about 5 percent. The results at an a/t ratio of 0.05 were very nearly equal to the asymptotic values at a/t = 0. For remote bending loading and

all crack shapes (a/c), lower values of a/t gave higher stress-intensity factors all along the crack front. This was expected because the crack experiences a more uniform stress gradient as a/t approaches zero. The asymptotic limits of the stress-intensity factors (as a/t approaches zero) given the empirical equations proposed by Newman and Raju were within 3 percent of the limits obtained by the finite-element method.

The stress-intensity factors given in this paper should be useful in predicting crack-growth rates and fracture strengths, in designing structural components, and in establishing inspection intervals for surface- and corner-cracked components.

ACKNOWLEDGEMENT

The first author's contribution to this work was performed under NASA contract NAS1-18256 at the NASA Langley Research Center, Hampton ,Va.

REFERENCES

[1] Gran, R. J., Orazio, F. D., Paris, P. C., Irwin, G. R., and Hertzberg, R. H., "Investigation and Analysis Development of Early Life Aircraft Structural Failures", AFFL-TR-70-149, Air Force Flight Laboratory, 1971.

[2] Raju, I. S. and Newman, J. C., Jr., "Stress-Intensity Factors for a Wide Range of Semi-Elliptical Surface Cracks in Finite-Thickness Plates," Engineering Fracture Mechanics, Vol. 11, No. 4, 1979, pp. 817-829.

[3] Newman, J. C, Jr. and Raju, I. S.,"Analyses of Surface Cracks in Finite Plates under Tension or Bending Loads," NASA TP-1578, 1979.

[4] Raju, I. S. and Newman, J. C., Jr., "Finite-Element Analysis of Corner Cracks in Rectangular Bars," NASA TM-89070, 1987.

[5] Heliot, J., Labbens, R. C., and Pellissier-Tanon, A., "Semi-elliptical Surface Cracks Subjected to Stress Gradients", in Fracture Mechanics, C. W. Smith (Ed), ASTM STP 677, American Society for Testing of Materials, 1979, pp. 341-364.

[6] Shah, R. C., and Kobayashi, A. S., " On the Surface Flaw Problem", In the Surface Crack: Physical Problems and Computational Solutions, J. L. Swedlow (Ed), ASME, American Society of Mechanical Engineers, 1972, pp. 79-142.

[7] Smith, F. W., " The Elastic Analysis of the Part-circular Surface Flaw Problem by the Alternating Method," In the Surface Crack: Physical Problems and Computational Solutions, J. L. Swedlow (Ed), ASME, American Society of Mechanical Engineers, 1972, pp. 125-152.

[8] Smith, F. W., and Kullgren, T. E., " Theoretical and Experimental Analysis of Surface Cracks Emanating from Fastener Holes", AFFDL-TR-76-104, Air Force Flight Dynamics Laboratory, 1977.

[9] Newman, J. C., Jr. and Raju, I. S., "Stress-Intensity Factor Equations for Cracks in Three-Dimensional Finite Bodies," Fracture Mechanics: Fourteenth Symposium - Volume I: Theory and Analysis, ASTM STP-791, J. C. Lewis and G. Sines, Eds., American Society for Testing and Materials, 1983, pp. I-238 - I-265.

[10] Newman, J. C. Jr., and Raju, I. S., "Stress-intensity Factor Equations for Cracks in Three-dimensional Finite Bodies Subjected to Tension and Bending Loads", Chapter 9, In Computational Methods in the Mechanics of Fracture, S. N. Atluri (Ed), North Holland, 1986, pp 312-334.

[11] Nishioka, T., and Atluri, S. N., "Analytical Solution for Embedded Elliptical Cracks, and Finite Element-Alternating Method for

Elliptical Surface Cracks, Subjected to Arbitrary Loadings," Engineering Fracture Mechanics, Vol 17, 1983, pp 247-268.

[12] Nishioka, T., and Atluri, S. N., "An Alternating Method for Analysis of Surface Flawed Aircraft Structural Components", AIAA Jnl., Vol. 21, 1983, pp. 749-757.

[13] Atluri, S. N., and Nishioka, T., " Computational Methods for Three-dimensional Problems of Fracture", Chapter 7, In Computational Methods in Mechanics of Fracture, S. N. Atluri (Ed), North Holland, 1986, pp. 230-287.

[14] Shah, R. C., and Kobayashi, A. S., "Stress-Intensity Factors for an Elliptic Crack under Arbitrary Loading," Engineering Fracture Mechanics, Vol. 3, 1971, pp. 71-96.

[15] Vijayakumar, K., and Atluri, S. N., " An Embedded Elliptical Flaw in an Infinite Solid, Subject to Arbitrary Crack-Face Tractions," Trans. ASME, Series E, Jnl. of Applied Mechanics, Vol. 48, 1981, pp. 88-96.

[16] Hinton, E., and Campbell, J. S., " Local and Global smoothing Discontinuous Finite Element Functions Using Least Squares Method", Int. Jnl. Num. Meth. Engng., Vol 8, 1974, pp. 461-480.

[17] Hinton, E., Scott, F. C., and Rickets, R. E., " Local Least Squares Stress Smoothing for Parabolic Isoparametric Elements", Int. Jnl. Num. Meth. Engng., Vol. 9, 1975, pp. 235-256.

Table 1.- Average normalized residual pressure on the crack face from mapped models.

Iteration Number	Finite-element model		
	Coarse	Medium	Fine
1	0.975	0.975	0.975
2	0.215	0.201	0.199
3	0.034	0.044	0.043
4	0.013	0.017	0.017
5	0.002	0.003	0.003

Table 2.- Average normalized residual pressure on the crack face from the rectangular models.

Iteration Number	Finite-element model		
	Coarse	Medium	Fine
1	1.273	1.273	1.273
2	0.144	0.171	0.171
3	0.020	0.027	0.027
4	0.006	0.007	0.008

Table. 3: Comparison of asymptotic limits of the normalized stress-intensity factors, F, as a/t approaches zero, obtained by the finite-element analysis (average value of tension and bending loading) and the empirical equation.

$$K = S_i \, (\pi a/Q)^{1/2} \quad F$$

a/c	Surface Cracks			
	$2\,\phi/\pi = 0.125$		$2\,\phi/\pi = 1.0$	
	Finite-element Analysis	Empirical Equation	Finite-element Analysis	Empirical Equation
0.2	0.621	0.623	1.094	1.112
0.4	0.764	0.771	1.073	1.094
0.6	0.896	0.902	1.055	1.076
1.0	1.119	1.107	1.022	1.040
	Corner Cracks			
	$2\,\phi/\pi = 0.125$		$2\,\phi/\pi = 0.875$	
0.2	0.618	0.588	1.095	1.108
0.4	0.752	0.736	1.085	1.104
0.6	0.886	0.871	1.090	1.100
1.0	1.104	1.094	1.104	1.094

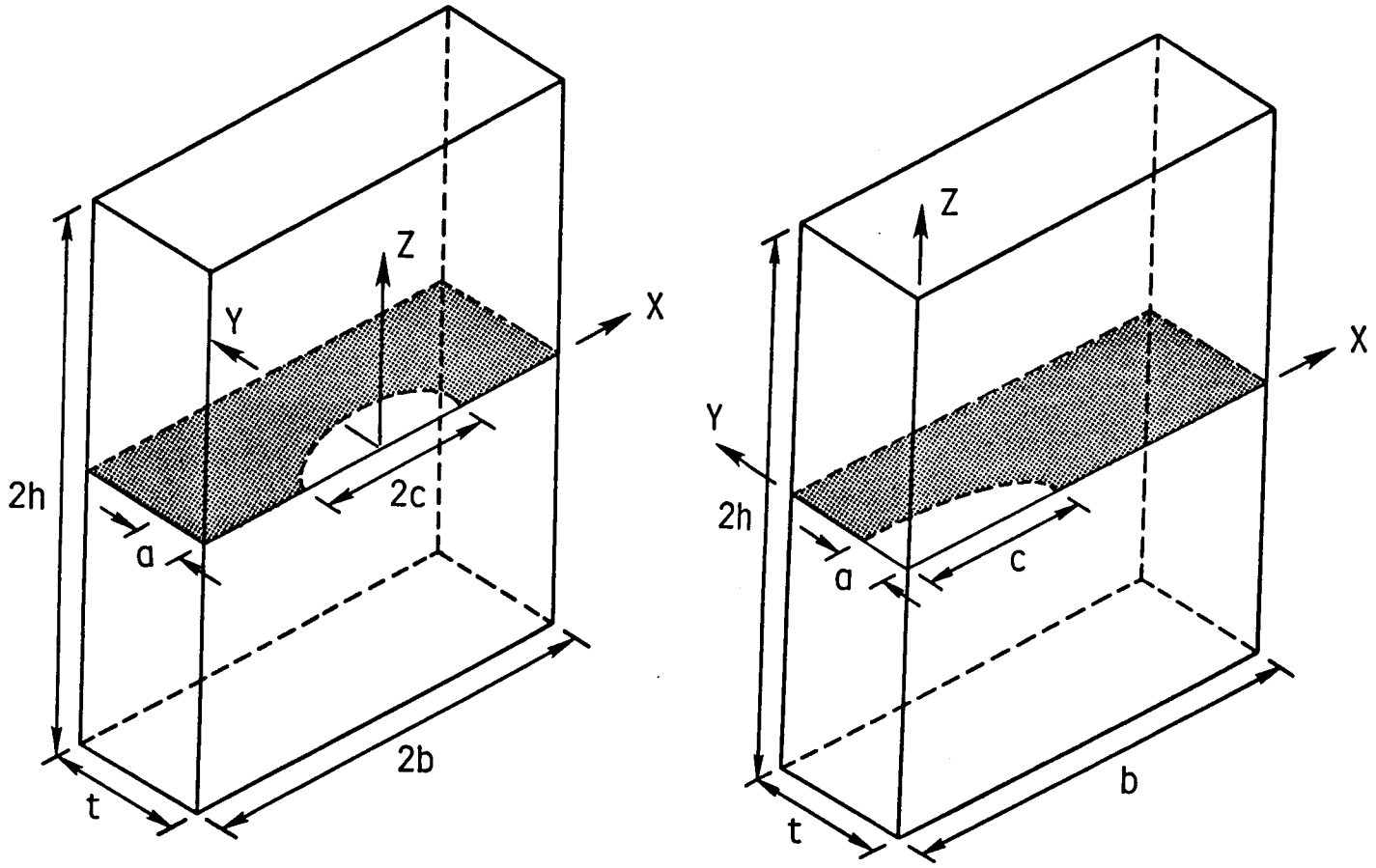

(a) Surface crack.

(b) Corner crack.

Figure 1.- Crack configurations analyzed.

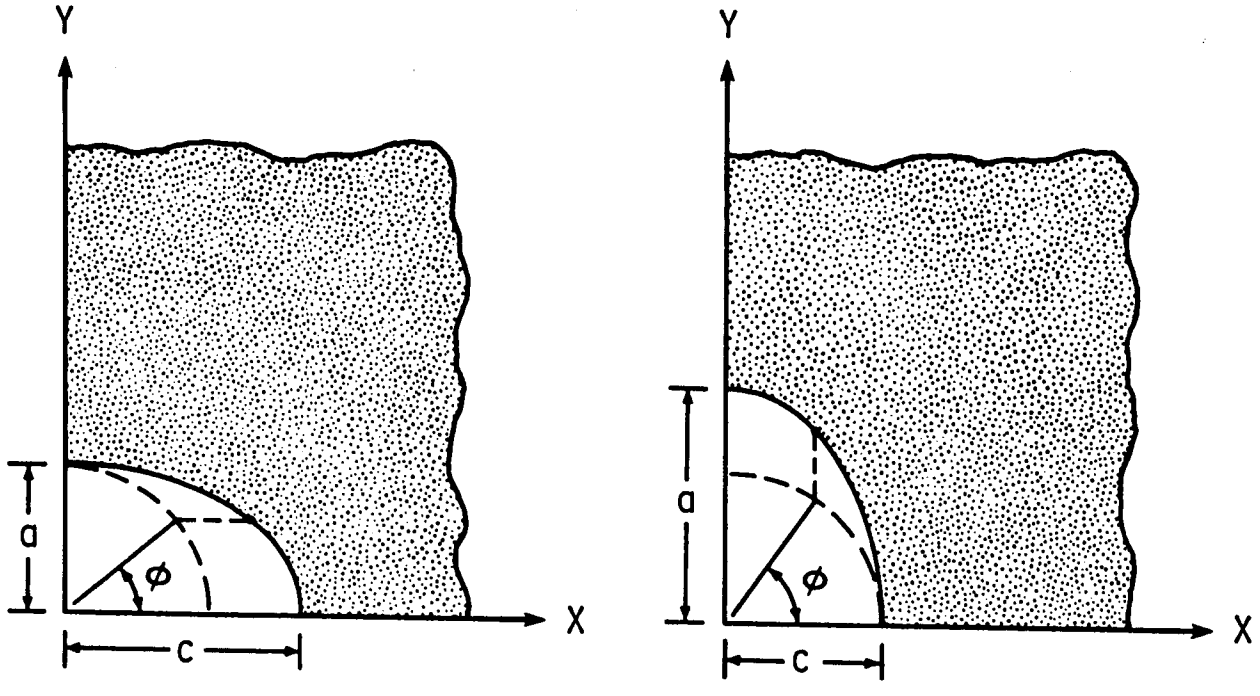

Figure 2.- Definition of parametric angle.

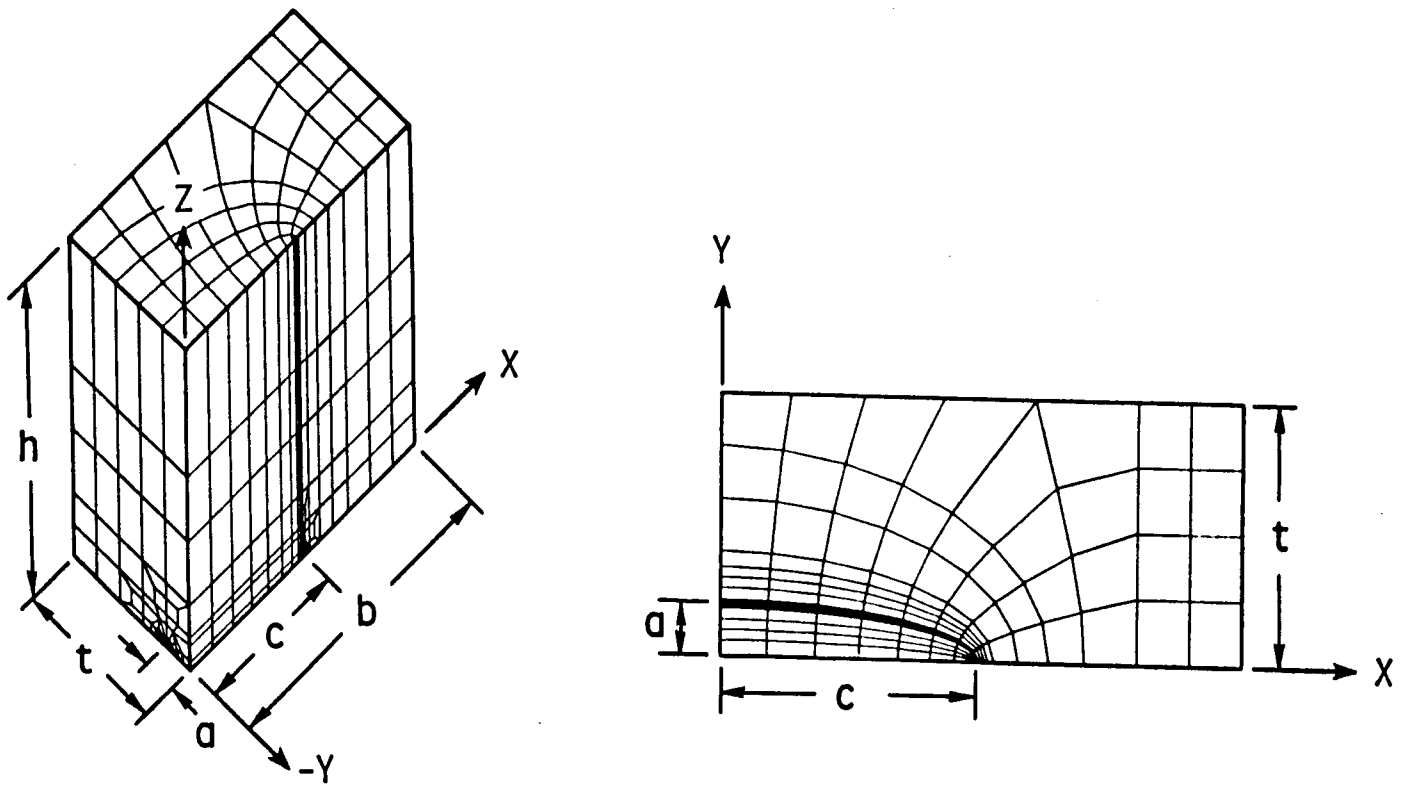

(a) Specimen model.

(b) Element pattern on Z = 0 plane.

Figure 3.- Finite-element model for surface- and corner-crack configuration.

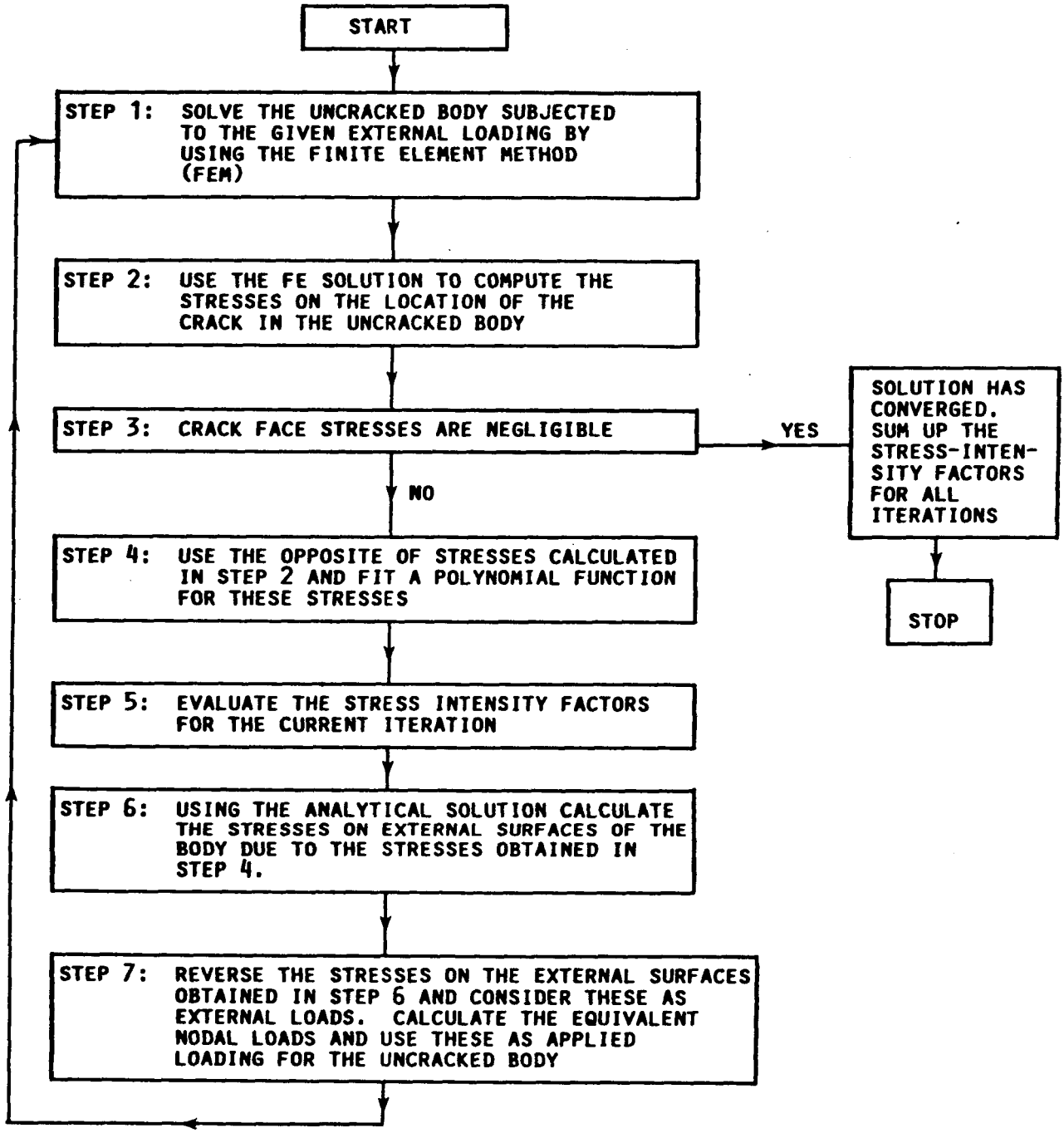

Figure 4.- Flow chart for the finite-element-alternating method.

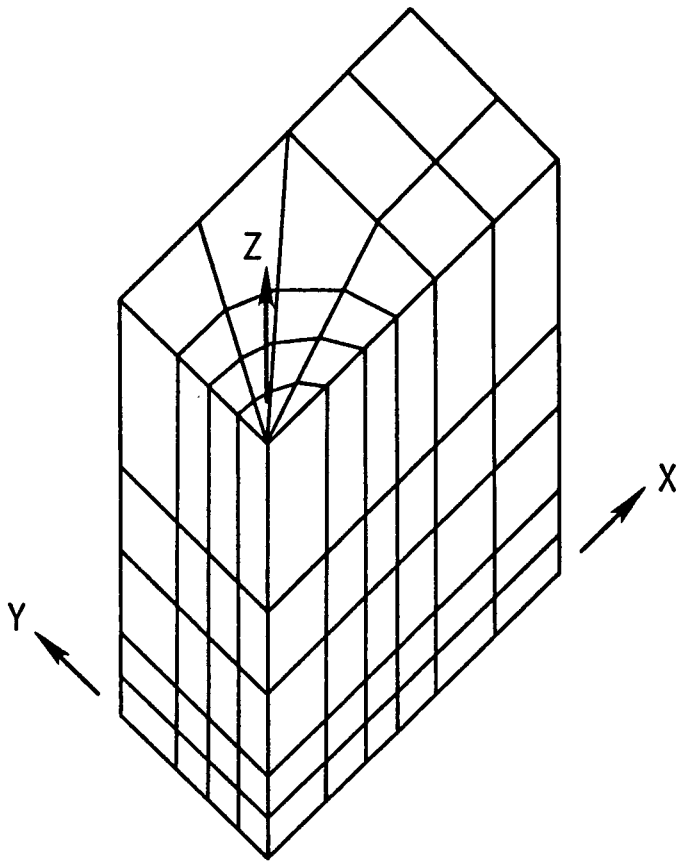

(a) Mapped model.

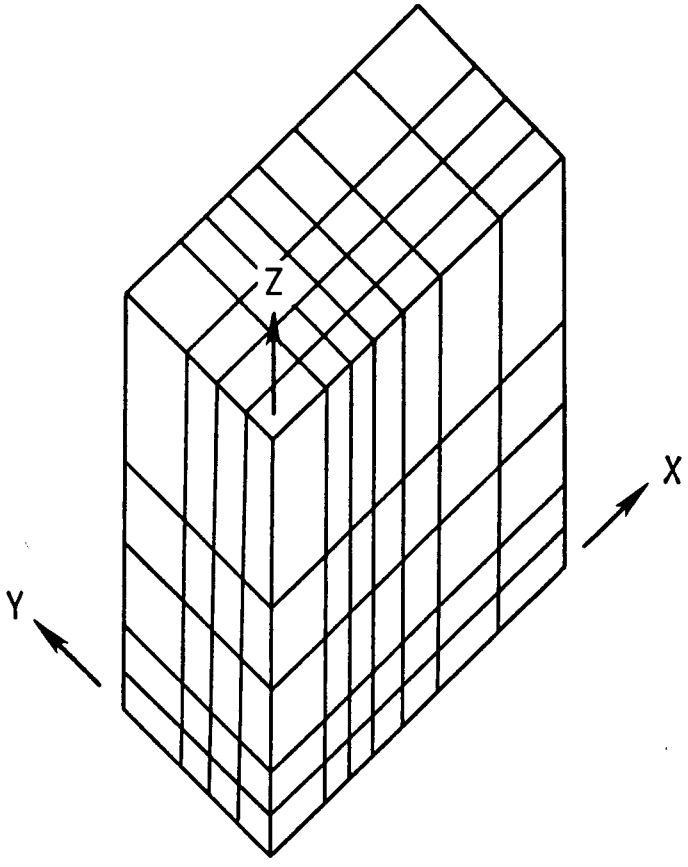

(b) Rectangular model.

Figure 5.- Finite-element models used in finite-element-alternating method.

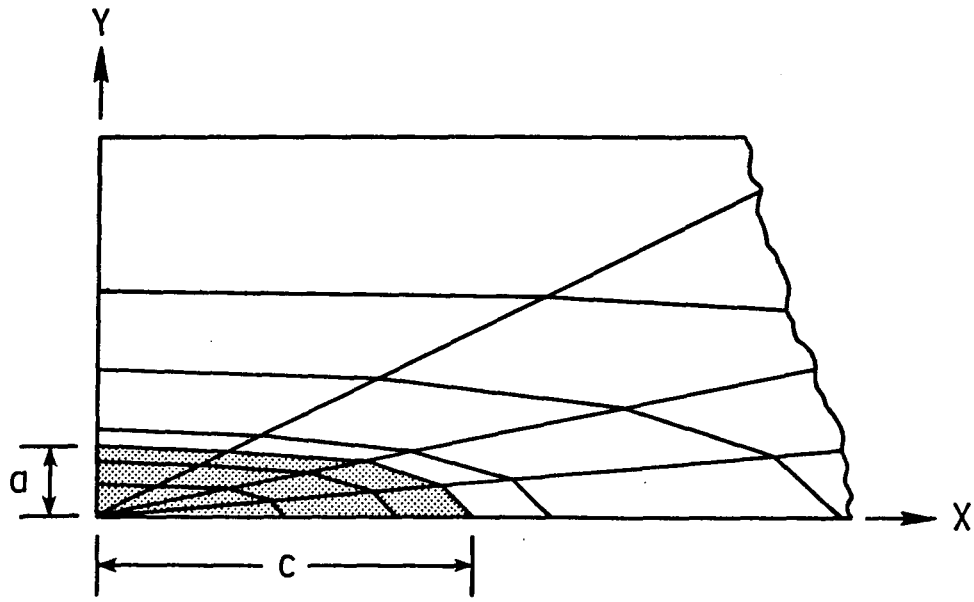

(a) Mapped model.

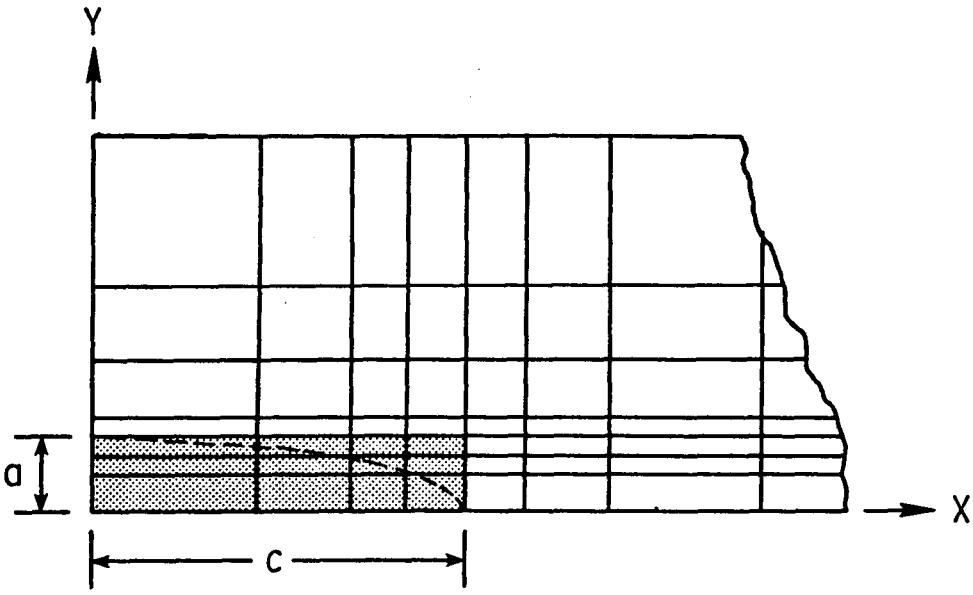

(b) Rectangular model.

Figure 6.- Crack-surface area used in residual pressure (σ_z^R) fit.

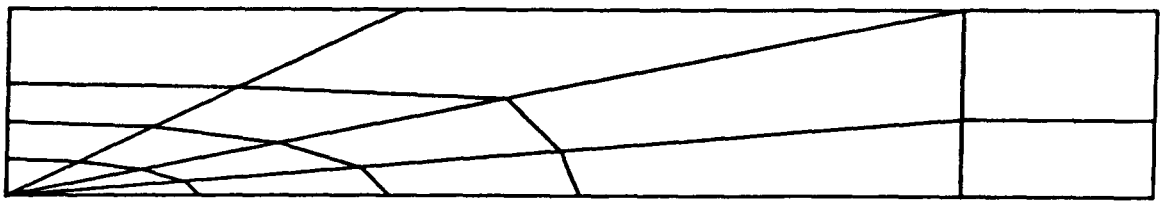

(a) Coarse mesh.

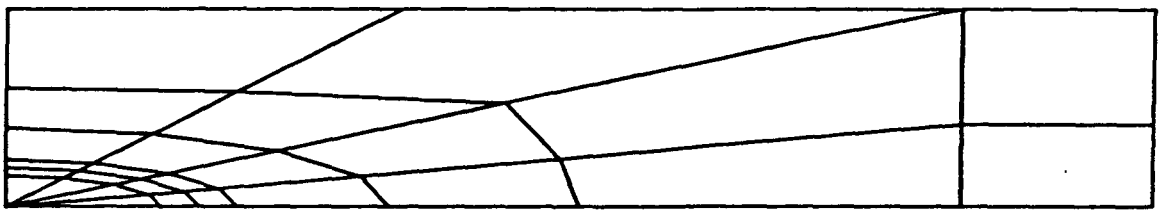

(b) Medium mesh.

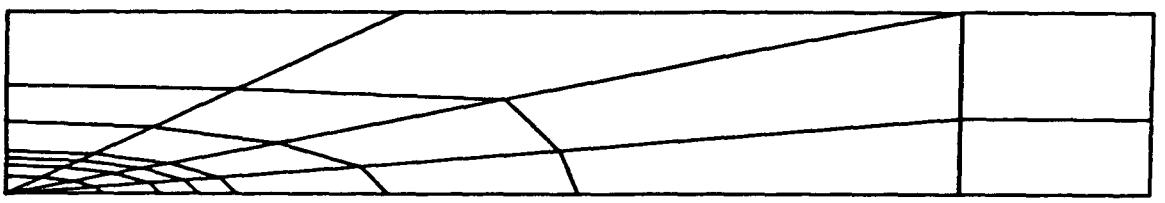

(c) Fine mesh.

Figure 7.- Mapped models used in finite-element-alternating method.

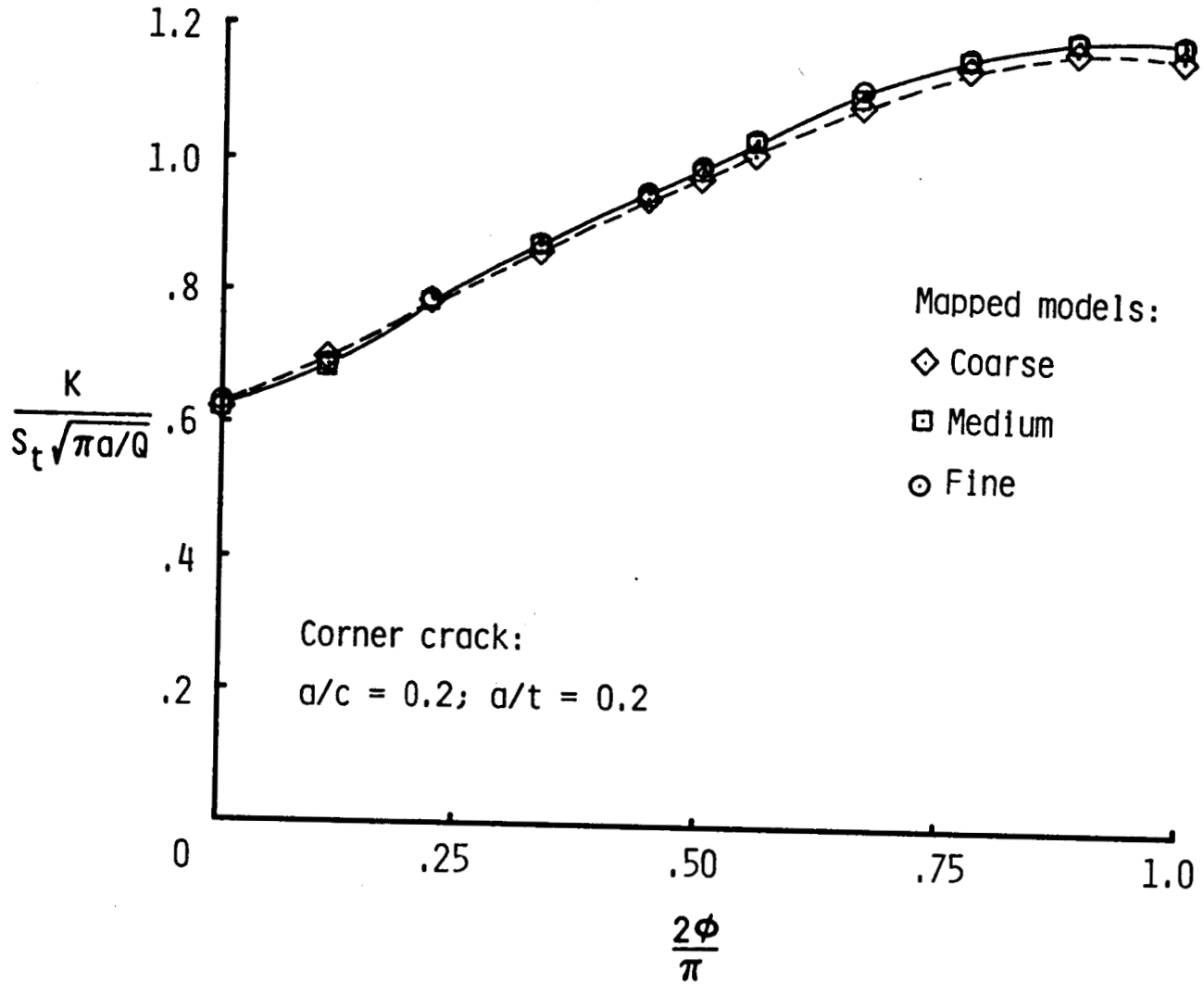

Figure 8.- Convergence of normalized stress-intensity factors from finite-element-alternating method using mapped models for quarter-elliptic corner crack in a plate under tension.

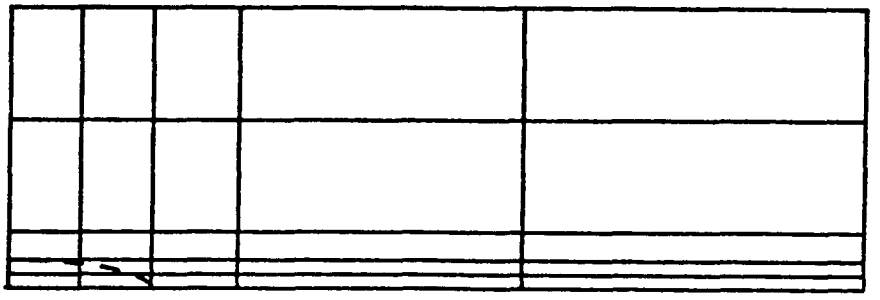

(a) Coarse mesh.

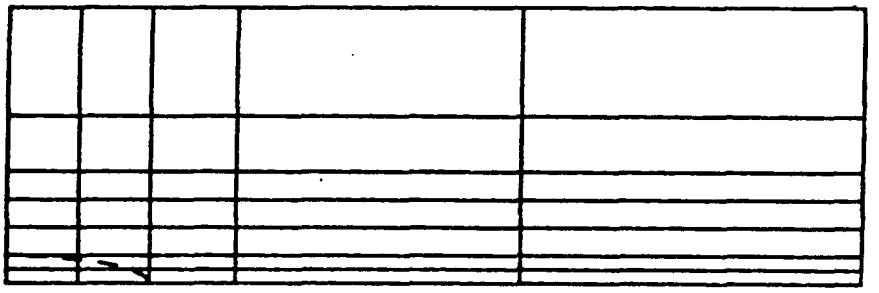

(b) Medium mesh.

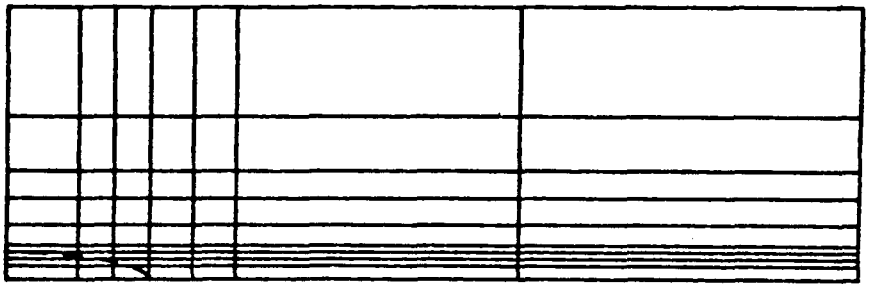

(c) Fine mesh.

Figure 9.- Rectangular models used in the finite-element-alternating method.

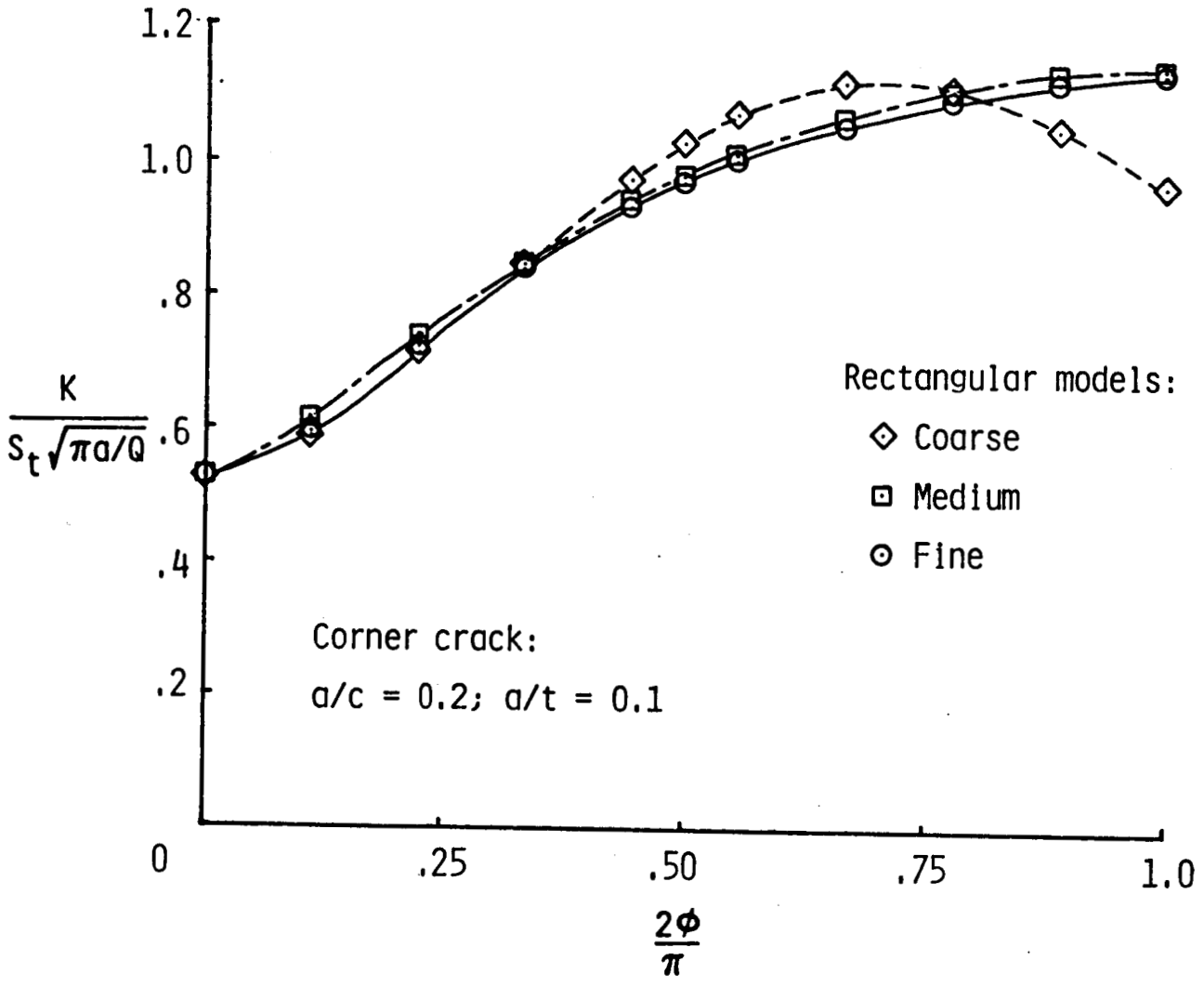

Figure 10.- Convergence of normalized stress-intensity factors from finite-element-alternating method using rectangular models for a quater-elliptic corner crack in a plate under tension.

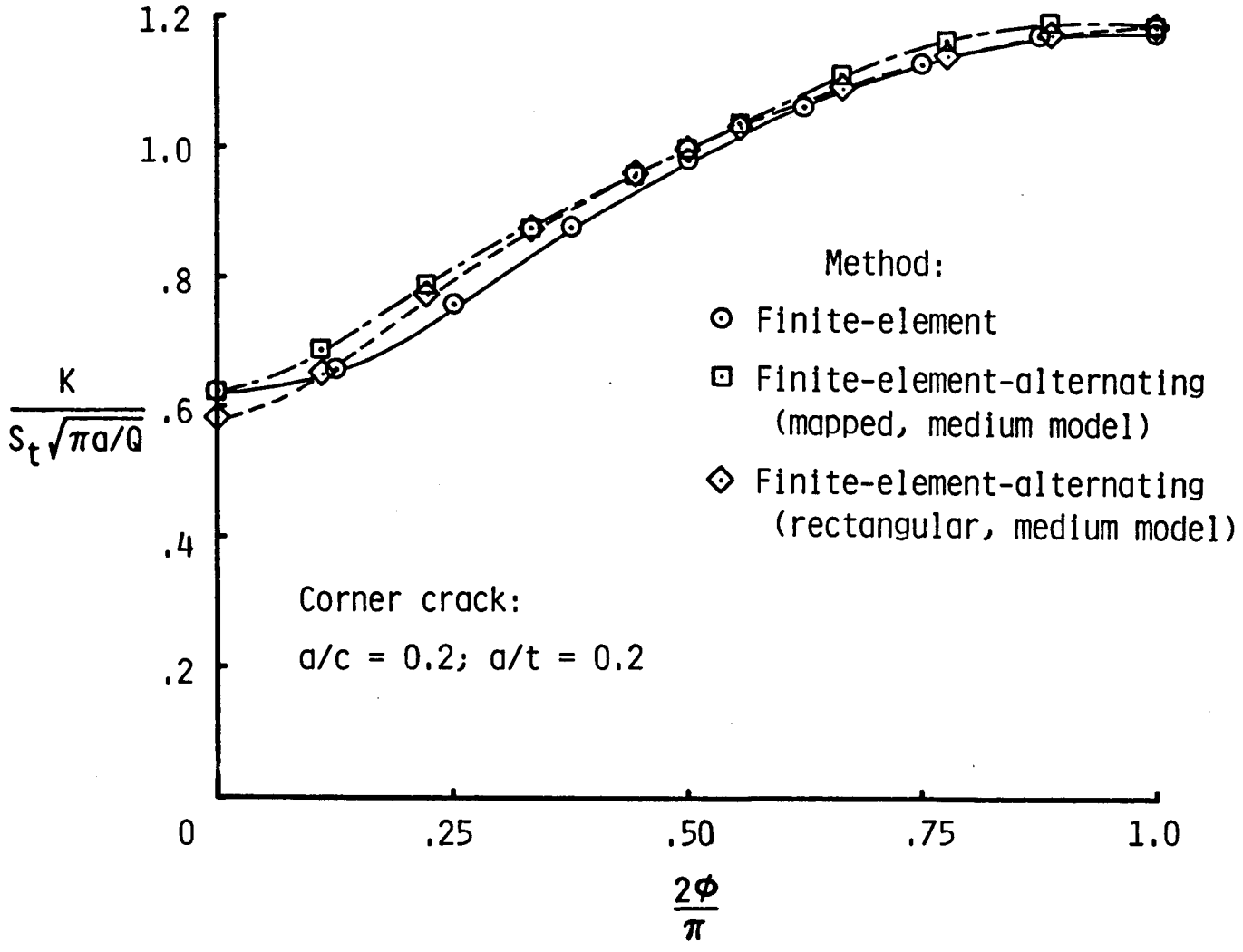

Figure 11.- Comparison of normalized stress-intensity factors from finite-element and finite-element-alternating methods for a quarter-elliptical corner crack in a plate under tension (a/c = 0.2; a/t = 0.2).

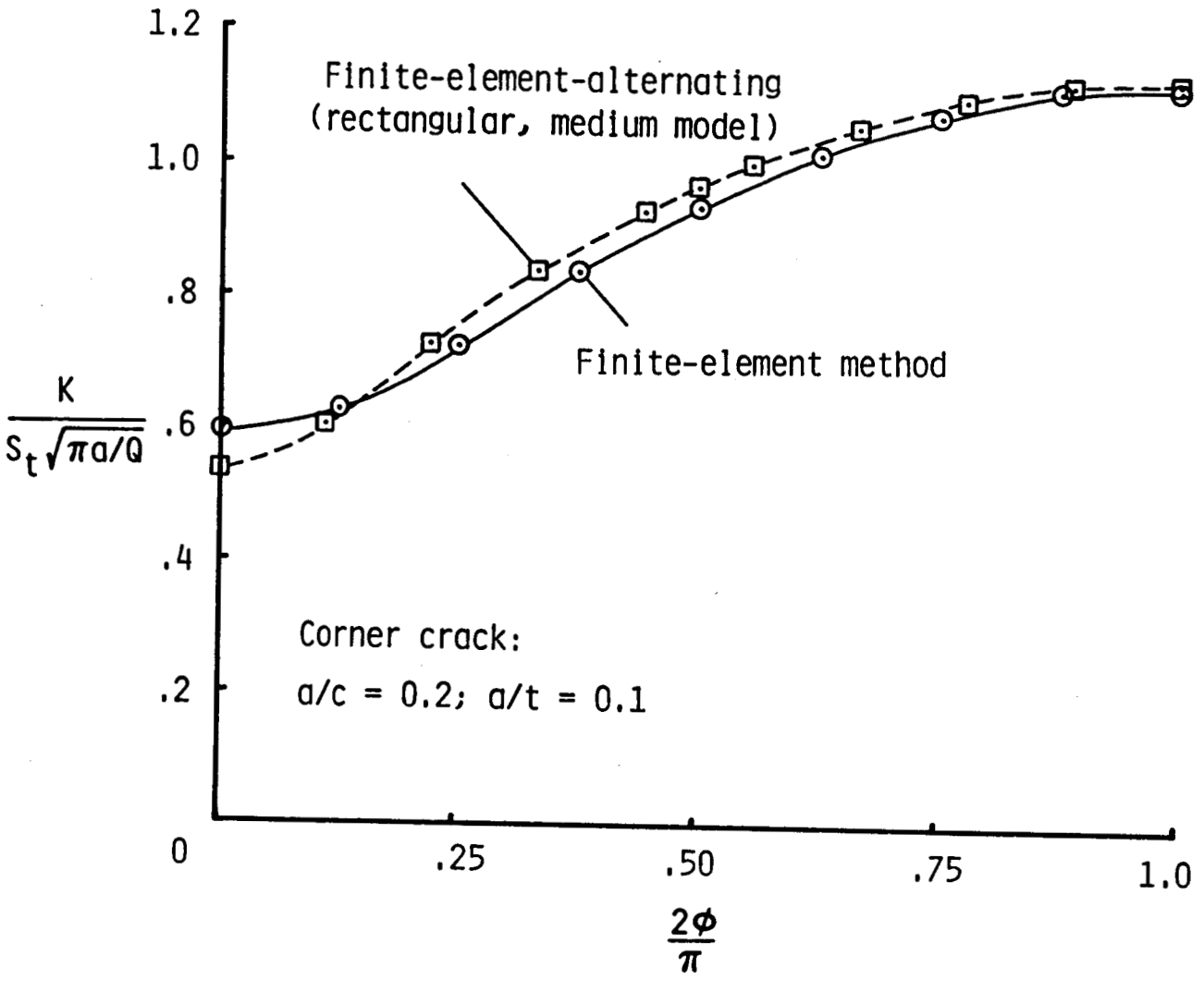

Figure 12.- Comparison of normalized stress-intensity factors from finite-element and finite-element-alternating methods for a quarter-elliptical corner crack in a plate under tension (a/c = 0.2; a/t = 0.1).

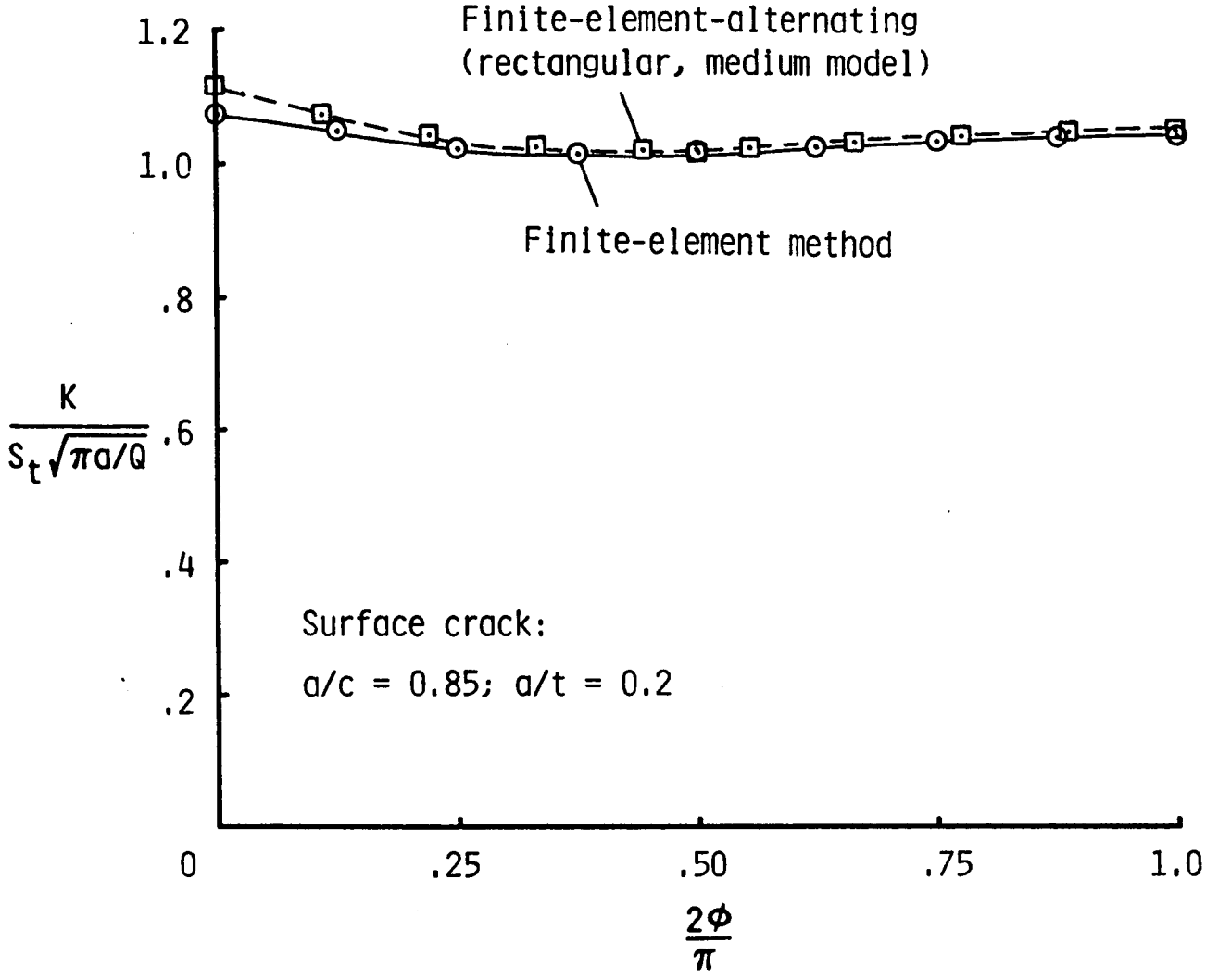

Figure 13.- Comparison of normalized stress-intensity factors from finite-element and finite-element-alternating methods for a near semi-circular surface crack under tension.

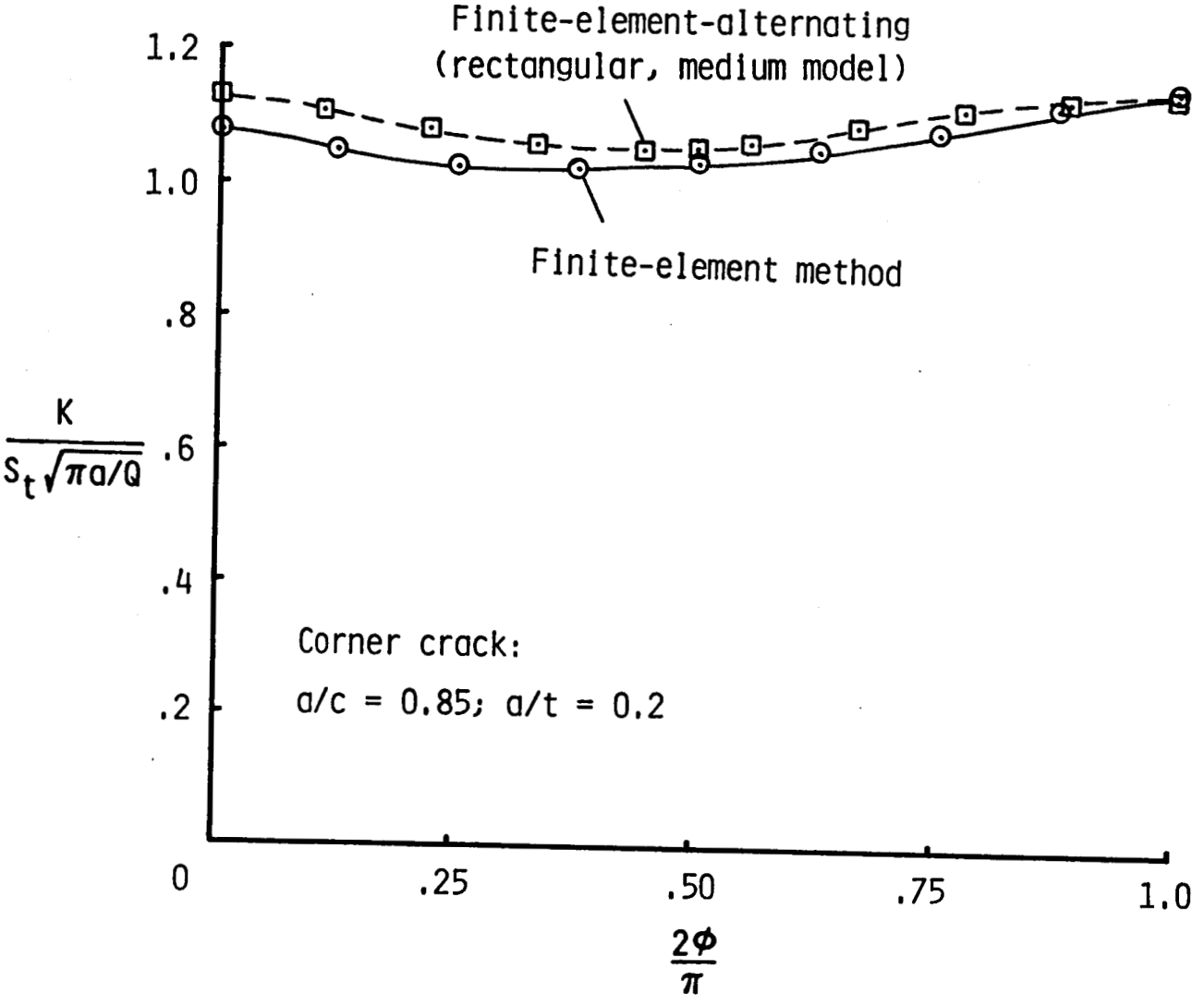

Figure 14.- Comparison of normalized stress-intensity factors from finite-element and finite-element-alternating methods for a near quarter-circular corner crack under tension.

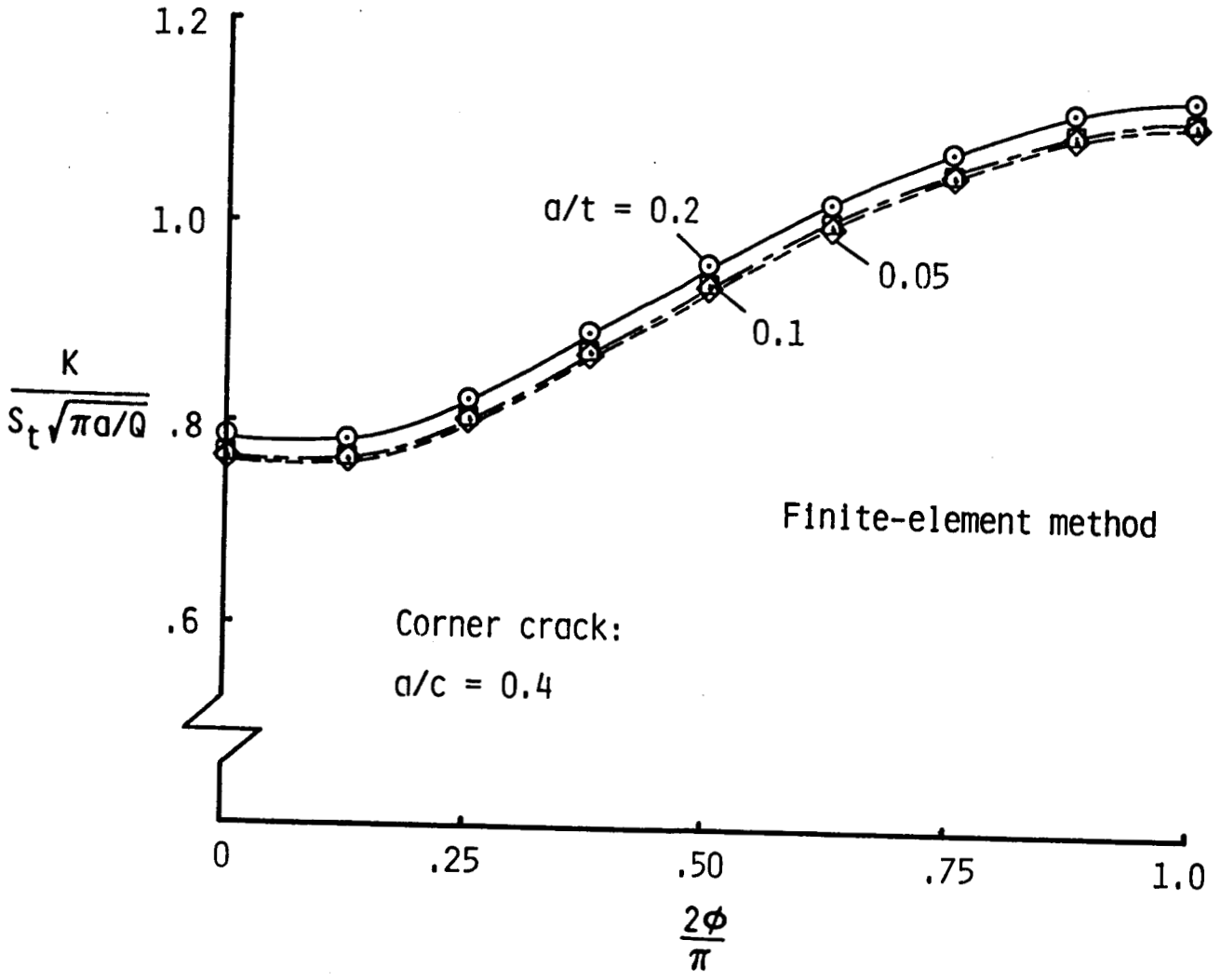

Figure 15.- Normalized stress-intensity factors for a quarter-elliptical corner crack (a/c = 0.4) in a plate under tension.

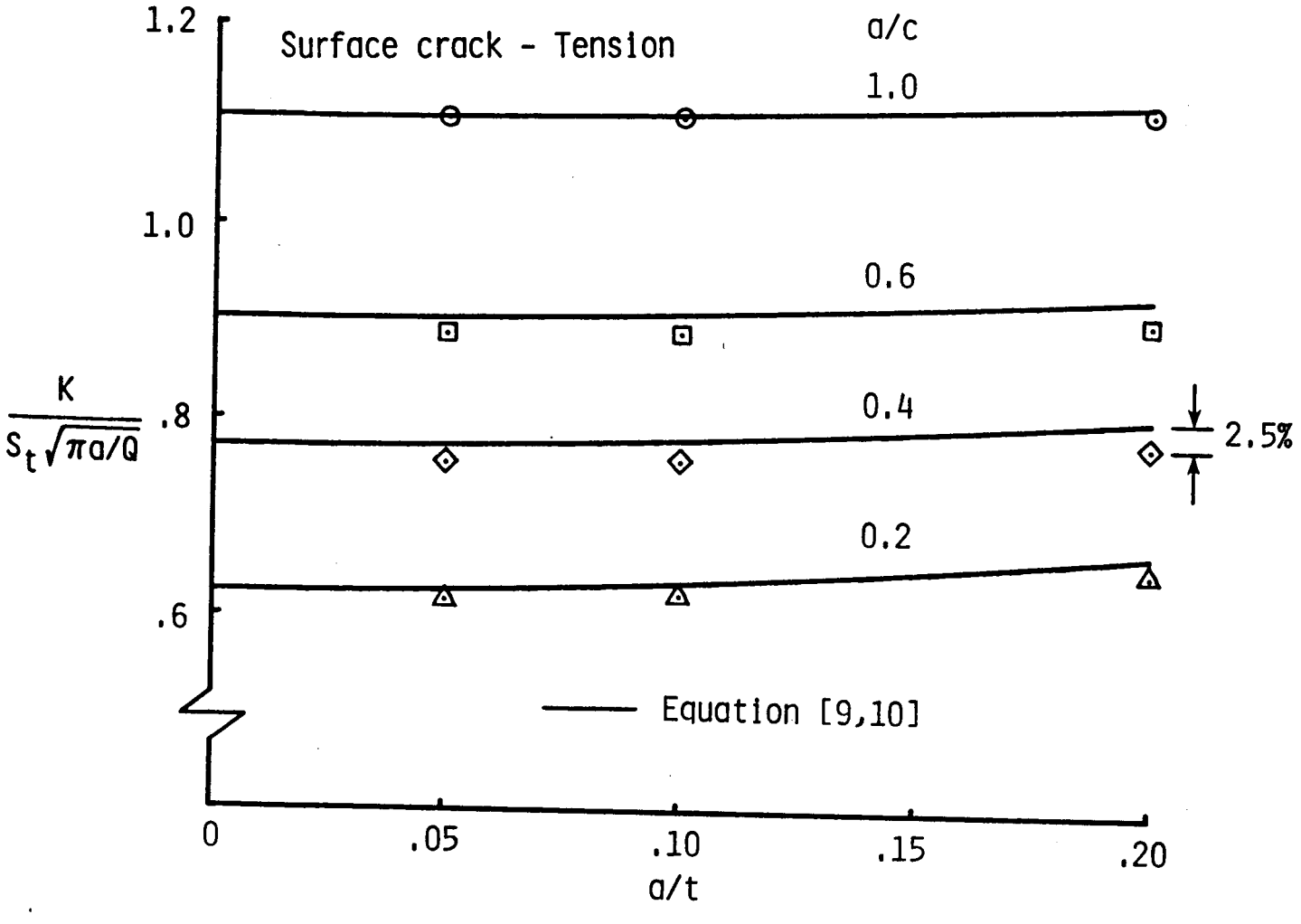

(a) At $2\phi/\pi = 0.125$.

Figure 16.- Comparisons of normalized stress-intensity factors from finite-element method and empirical equations for surface cracks in a plate under tension.

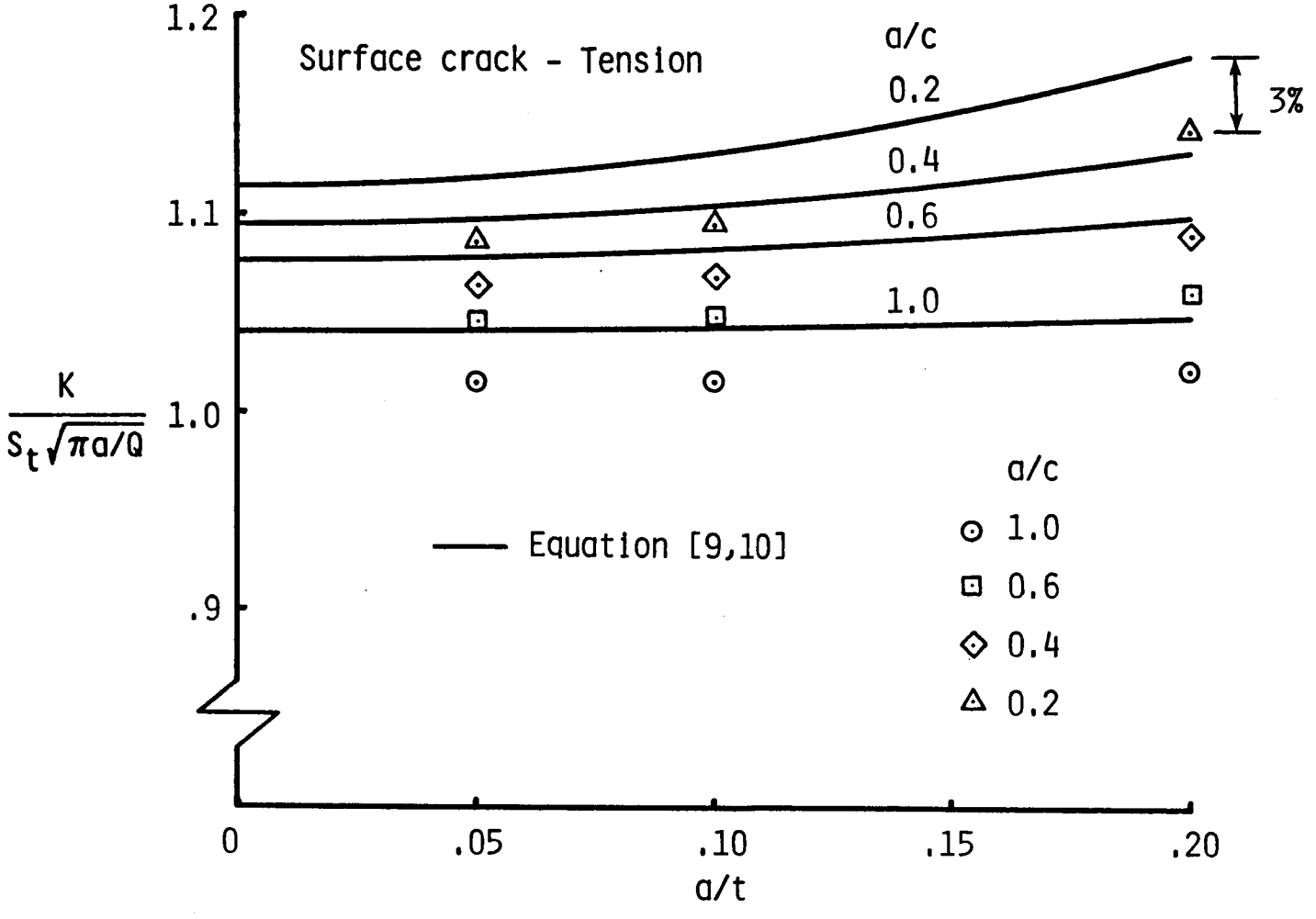

(b) At $2\phi/\pi = 1$.

Figure 16.- continued.

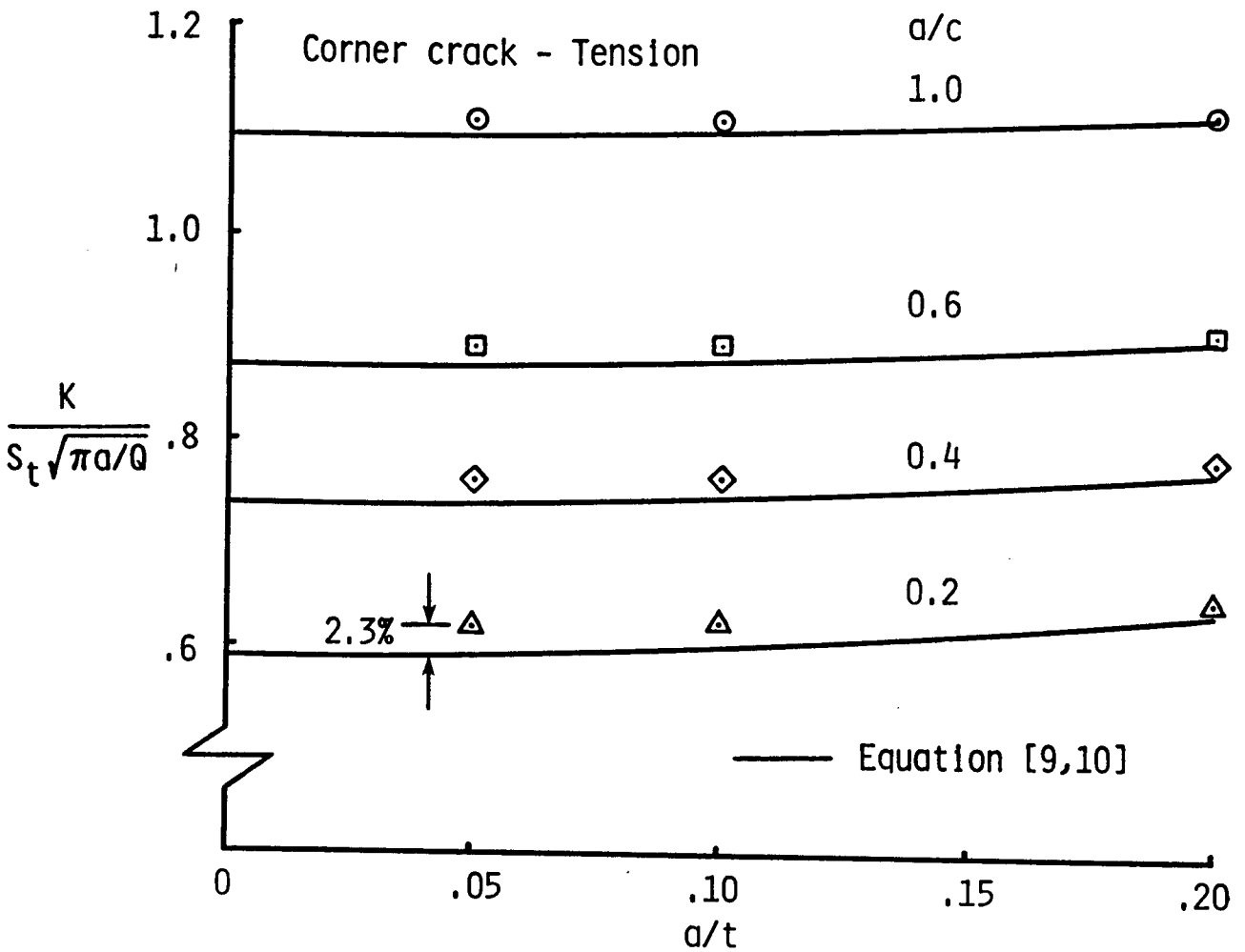

(a) At $2\phi/\pi = 0.125$.

Figure 17.- Comparisons of normalized stress-intensity factors from finite-element method and empirical equations for corner cracks in a plate under tension.

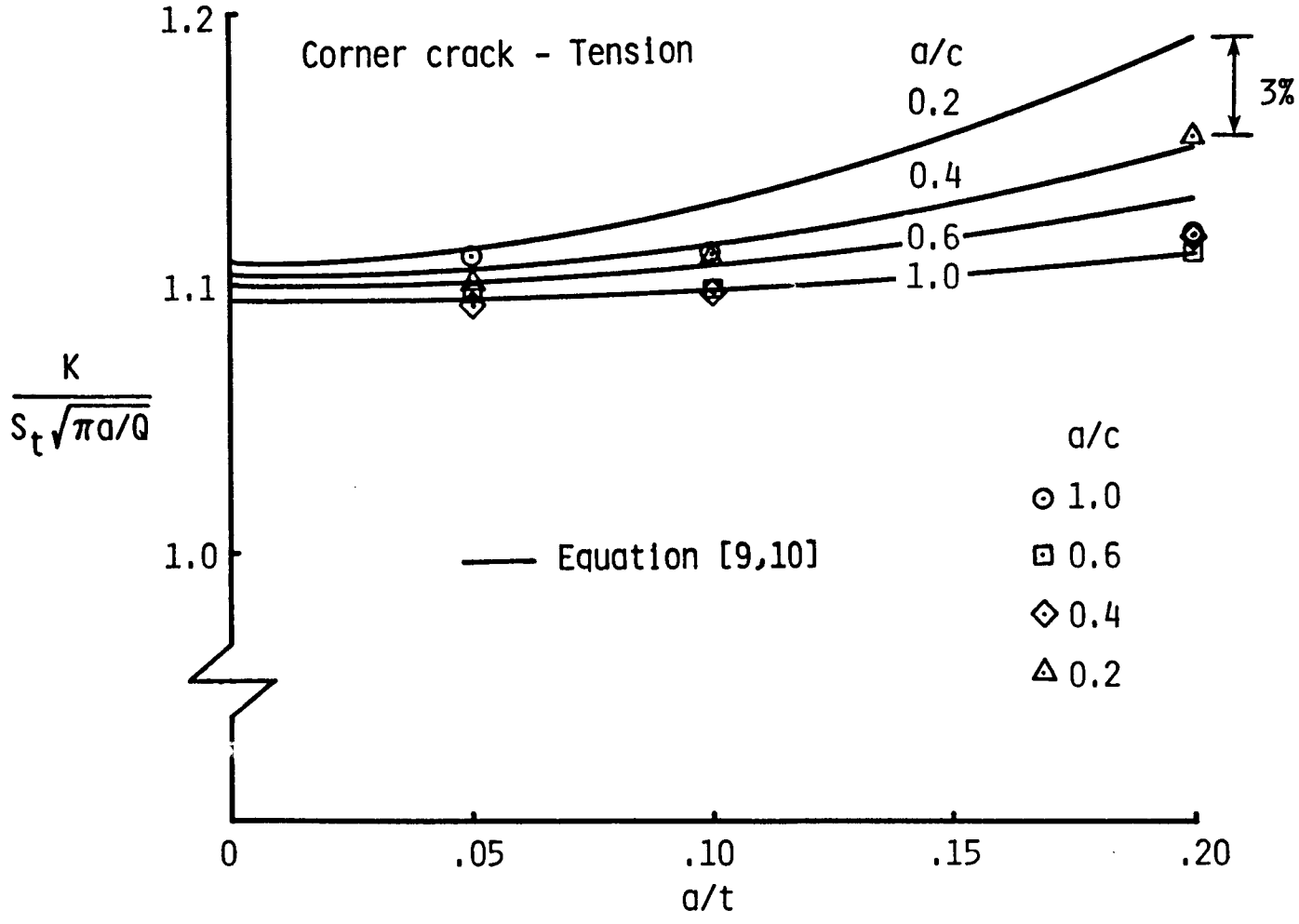

(b) At $2\phi/\pi = 0.875$.

Figure 17.- continued.

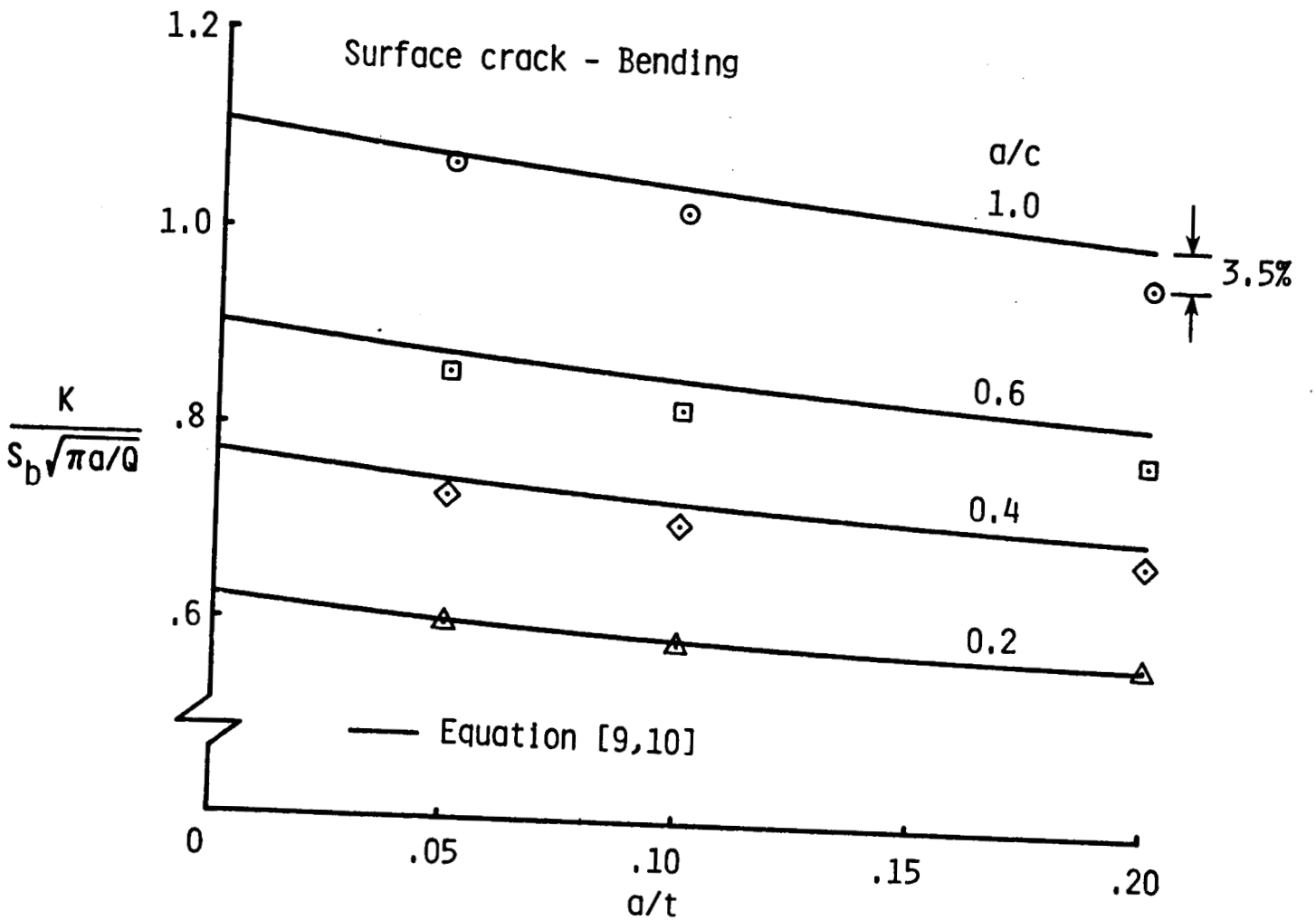

(a) At $2\Phi/\pi = 0.125$.

Figure 18.- Comparisons of normalized stress-intensity factors from finite-element method and empirical equations for surface cracks in a plate under bending.

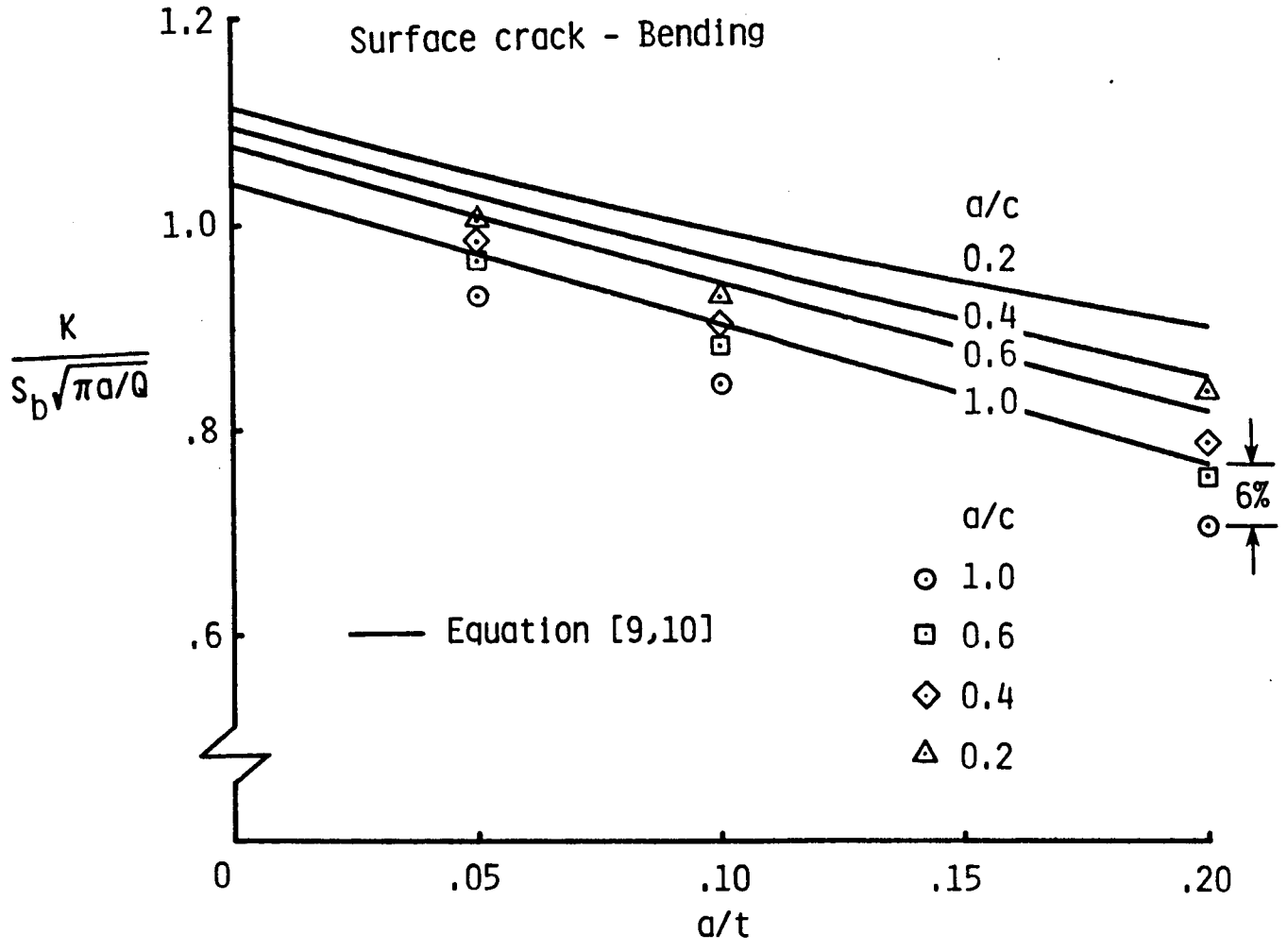

(b) At $2\phi/\pi = 1$.

Figure 18.- continued.

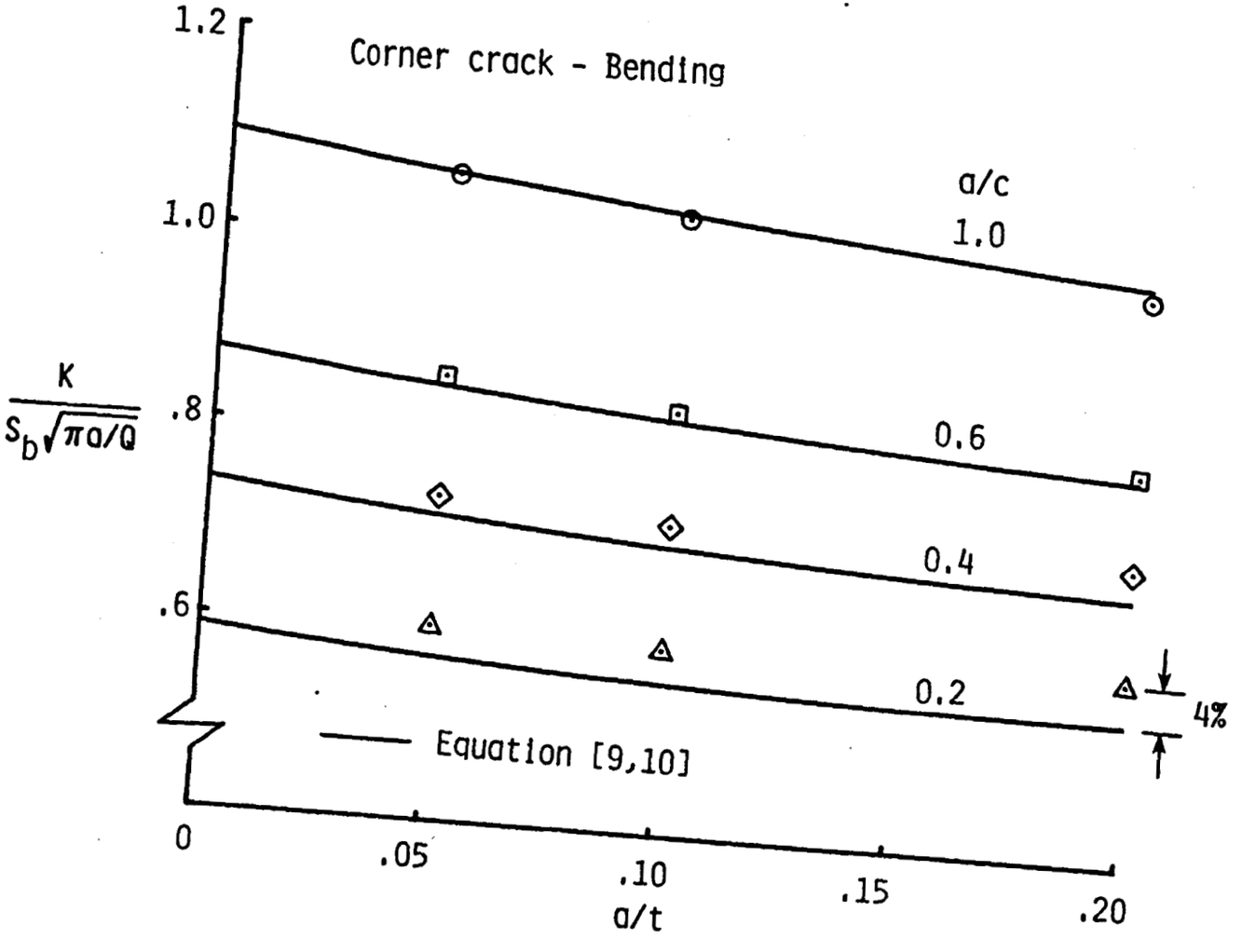

(a) At $2\phi/\pi = 0.125$.

Figure 19.- Comparisons of normalized stress-intensity factors from finite-element method and empirical equations for corner cracks in a plate under bending.

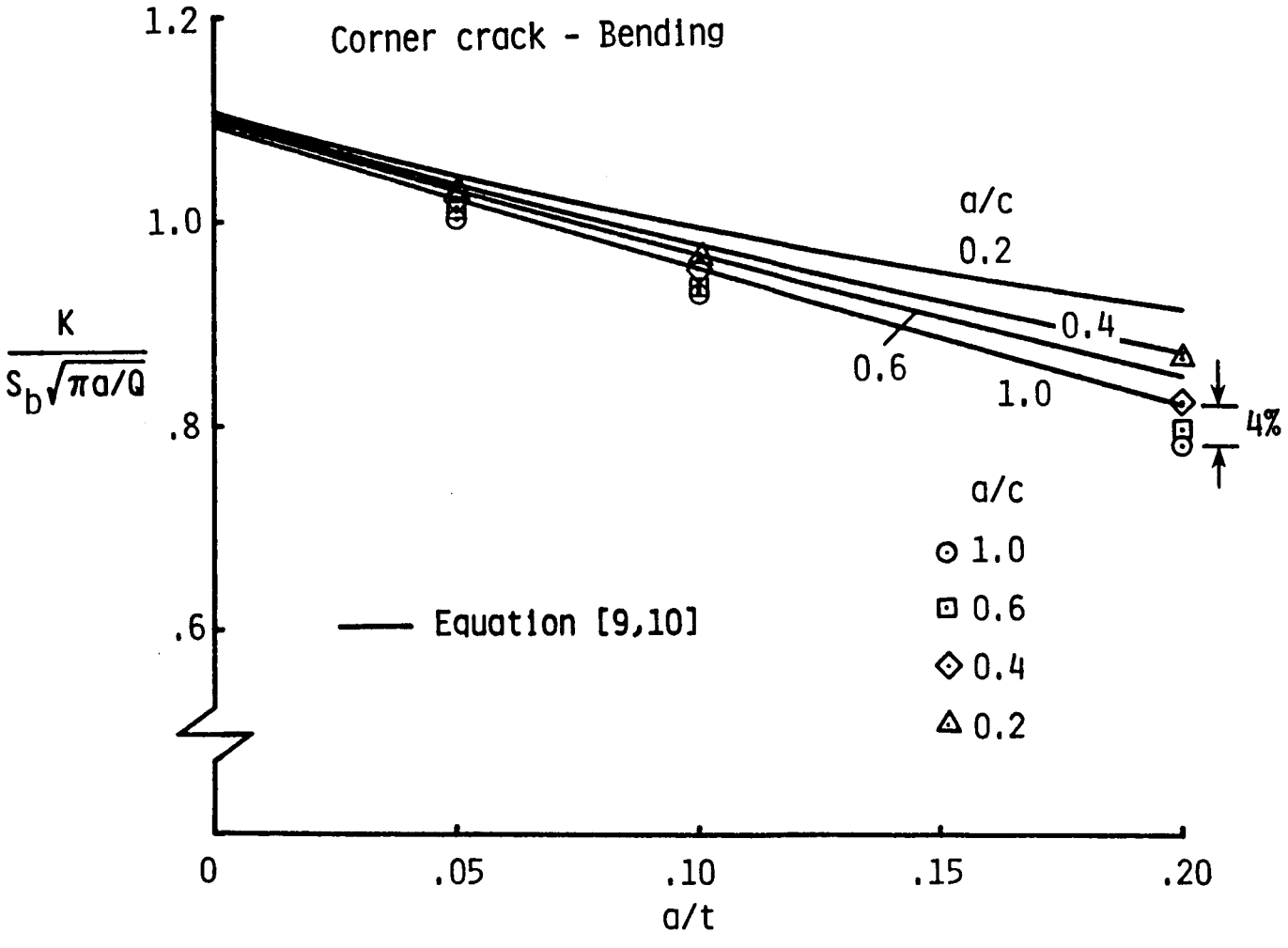

(b) At $2\phi/\pi = 0.875$.

Figure 19.- continued.

Standard Bibliographic Page

1. Report No.	2. Government Accession No.	3. Recipient's Catalog No.
NASA TM-100599		

4. Title and Subtitle	5. Report Date
Stress-Intensity Factors for Small Surface and Corner Cracks in Plates	April 1988
	6. Performing Organization Code
7. Author(s)	8. Performing Organization Report No.
I. S. Raju, S. N. Atluri, and J. C. Newman, Jr.	
9. Performing Organization Name and Address	10. Work Unit No.
NASA Langley Research Center Hampton, VA 23665-5225	505-63-01-05
	11. Contract or Grant No.
12. Sponsoring Agency Name and Address	13. Type of Report and Period Covered
National Aeronautics and Space Administration Washington, DC 20546-0001	Technical Memorandum
	14. Sponsoring Agency Code

15. Supplementary Notes

I. S. Raju, Analytical Services and Materials, Inc., Hampton, VA 23666;
S. N. Atluri, Georgia Institute of Technology, Atlanta, GA 30332; and
J. C. Newman, Jr., Langley Research Center, Hampton, VA 23665

16. Abstract

Three-dimensional finite-element and finite-element-alternating methods were used to obtain the stress-intensity factors for small surface and corner cracked plates subjected to remote tension and bending loads. The crack-depth-to-crack-length ratios (a/c) ranged from 0.2 to 1 and the crack-depth-to-plate-thickness ratios (a/t) ranged from 0.05 to 0.2. The performance of the finite-element alternating method was studied on these crack configurations. A study of the computational effort involved in the finite-element alternating method showed that several crack configurations could be analyzed with a single rectangular mesh idealization, whereas the conventional finite-element method requires a different mesh for each configuration. The stress-intensity factors obtained with the finite-element-alternating method agreed well (within 5 percent) with those calculated from the finite-element method with singularity elements.

The stress-intensity factors calculated from the empirical equations proposed by Newman and Raju were generally within 5 percent of those calculated by the finite-element method. The stress-intensity factors given herein should be useful in predicting crack-growth rates and fracture strengths of surface- and corner-cracked components.

17. Key Words (Suggested by Authors(s))	18. Distribution Statement
Crack Elastic analysis Stress-intensity factor Finite-element method Finite-element-alternating method Surfact crack	Unclassified - Unlimited Subject Category - 39

19. Security Classif.(of this report)	20. Security Classif.(of this page)	21. No. of Pages	22. Price
Unclassified	Unclassified	45	A03

For sale by the National Technical Information Service, Springfield, Virginia 22161